MECHANISMS MEDIATING LOCAL GENERATION OF THETA-FREQUENCY EEG ACTIVITY IN THE SUPERFICIAL LAYERS OF THE PARASUBICULUM

Stephen D. Glasgow

A Thesis in

The Department of

Psychology

Presented in Partial Fulfillment of the Requirements

for the Degree of Master of Arts at Concordia University

Montréal, Québec

July, 2006

Your file Votre référence
ISBN: 978-0-494-20691-1
Our file Notre référence
ISBN: 978-0-494-20691-1

ABSTRACT

Mechanisms Mediating Local Generation of Theta-Frequency EEG Activity in the Superficial Layers of the Parasubiculum

Stephen D. Glasgow

The parasubiculum is a major component of the subicular complex, and plays an integral role in the retrohippocampal circuitry. It receives numerous inputs from the hippocampus, medial septum, thalamus, and other subcortical areas, and sends its major output projection to the layer II of the medial entorhinal cortex. Theta-frequency EEG activity (4-12 Hz) is a sinusoidal-like waveform, and has been correlated with numerous cognitive processes. The present studies were aimed at determining whether the superficial layers of the parasubiculum generate theta-frequency EEG activity locally, and whether membrane potential oscillations in parasubicular neurons may contribute to the generation of theta activity in this area. In the urethane-anaesthetized rat, cholinergically-mediated theta activity was recorded as a bipolar electrode passed through the superficial layers of the parasubiculum, and the theta activity was phase-locked to theta activity recorded in the stratum radiatum/lacunosum-moleculare of the hippocampal CA1 region. Using whole-cell current-clamp recordings in acute brain slices, voltage-dependent theta-frequency membrane potential oscillations were observed in the majority of layer II parasubicular neurons when the cells were held near threshold voltages using steady current injection. The frequency of oscillations increased when the cells were heated from 22°C to 32°C, and persisted in the presence of blockers of fast ionotropic glutamatergic and GABAergic synaptic transmission. The oscillations are therefore likely generated intrinsically by voltage-dependent ionic conductances. These

results suggest that the superficial layers of the parasubiculum locally generate theta-frequency EEG activity, and that voltage-dependent membrane potential oscillations may contribute to the generation of this activity *in vivo*.

ACKNOWLEDGEMENTS

First and foremost, I would like to thank Dr. C. Andrew Chapman for his support, patience (answering innumerable tedious questions), and insight. I would also like to thank Douglas Caruana for the many useful discussions regarding all aspects of the hippocampal formation, and electrophysiology in general. Additionally, I would like to thank the members of my committee, Dr. Shimon Amir and Dr. Jim Pfaus, for their comments on an earlier draft of this manuscript, as well as discussions relating the significance of this work to a more global understanding of the brain. I would also like to thank my family (my mother, Susan; and sisters Mag and Jen) for their endless love and support over the years. Finally, I would like to thank the countless number of people who have endured my ramblings about theta and the parasubiculum over the past two years. The research presented here was supported by grants to C. A. Chapman from the Natural Sciences and Engineering Research Council of Canada, the Fonds pour la Formation de Chercheurs et à la Recherche, and the Canadian Foundation for Innovation.

TABLE OF CONTENTS

LIST OF FIGURES

LIST OF ABBREVIATIONS

ACSF	Artificial cerebrospinal fluid
AMPA	amino-3-hydroxy-5-methyl-isoxazole-propinoic acid
ANOVA	Analysis of variance
AP-5	DL-(±)-2-amino-5-phosphonopentanoic acid
ATP	Adenosine triphosphate
BIC	Bicuculline methiodide
CA	Cornu ammonis
Ca^{2+}	Calcium
$CaCl_2$	Calcium chloride
Cl	Chloride
CO_2	Carbon dioxide
DC	Direct current
EC	Entorhinal cortex
EEG	electroencephalography
EGTA	Ethylene glyco-bis (β-aminoethyl ether)-N,N,N',N'-tetraacetic acid
fAHP	Fast afterhyperpolarization
GABA	Gamma aminobuytric acid
GΩ	GigaOhm
GTP	Guanosine triphosphate

HEPES	N-2-hydroxyethylpiperazine-N'-2-ethanesulfonic acid
Hz	Hertz
I_a	Delayed inactivating transient potassium current
I_h	Hyperpolarization-activated non-specific cationic current
I_{Nap}	Persistent sodium current
K^+	Potassium
KCl	Potassium chloride
mAHP	Medium afterhyperpolarization
Mg^{2+}	Magnesium
$MgCl_2$	Magnesium chloride
$MgSO_4$	Magnesium sulfate
MΩ	MegaOhm
MPO	Membrane potential oscillations
mV	millivolts
Na^+	Sodium
NaCl	Sodium chloride
$NaHCO_3$	Sodium bicarbonate
NaH_2PO_4	Dibasic sodium phosphate
NBQX	1,2,3,4-tetrahydro-6-nitro-2,3-dioxo-benzo(f)quinoxaline-7-sulfonamide disodium
NMDA	N-methyl-D-aspartate
O_2	Oxygen

i.v.	intravenous
PaS	Parasubiculum

INTRODUCTION

The parasubiculum (PaS) is a major component of the hippocampal formation, and may play a substantial role in spatial navigation and formation of place cell representations (Hargreaves, Rao, Lee, & Knierim, 2005; Taube, 1995b). It receives major inputs from the hippocampus and medial septum with weaker inputs from the subiculum, basolateral amygdala, and anterior thalamus, and it sends its major output to layer II of the entorhinal cortex (EC) (Figure 1; Amaral & Witter, 1989; Caballero-Bleda & Witter, 1993, 1994; Funahashi & Stewart, 1997a; Swanson & Cowan, 1979; Wouterlood, Saldana, & Witter, 1990). Layer II of the EC carries the major cortical input to the dentate gyrus and CA3 region of the hippocampus, and the presence of major parasubicular inputs to layer II of the EC suggests that the PaS may affect processing of sensory and spatial information in the limbic system (Alonso & Garcia-Austt, 1987a; Dickson, Trepel, & Bland, 1994; Hafting, Fyhn, Molden, Moser, & Moser, 2005). Activation of parasubicular efferents to the EC can enhance or suppress responses of the EC to inputs from the piriform cortex, indicating that the PaS may also play a major role in modifying cortical sensory information that arrives in layer II (Caruana & Chapman, 2004). The facilitation or suppression of entorhinal responses by the PaS is strongly time-dependent, and responses in the EC are facilitated if the PaS is stimulated 20-150 ms prior to piriform stimulation. This finding suggests that synchronized rhythmic activity in the PaS may contribute to facilitation of synaptic responses in the EC. In order to fully understand the role of the PaS modulating the input of sensory information to the hippocampal formation, it is essential to understand the cellular and network mechanisms which contribute to the interaction of the PaS with other brain regions during

endogenous, synchronous neuronal population activities such as theta-frequency EEG activity (Bland & Oddie, 2001; Bland, Oddie, & Colom, 1999; Bonansco & Buno, 2003; Buzsaki, 2002; Buzsaki, Leung, & Vanderwolf, 1983; Kramis & Vanderwolf, 1980; L. S. Leung, 1998; Petsche, Stumpf, & Gogolak, 1962; Robinson, 1980). The objective of the present studies was to determine if theta-frequency EEG activity was generated in the superficial layers of the PaS, and to assess whether membrane potential oscillations contribute to the generation of theta in the PaS.

Hippocampal theta-frequency activity is the most prominent EEG waveform in the mammalian limbic system. The hippocampal theta rhythm is a large-amplitude, sinusoidal-like waveform (4-12 Hz) that represents synchronized neural activity, and that involves numerous brainstem, hippocampal and retrohippocampal areas (Bland & Oddie, 2001; Buzsaki, 2002; Green & Arduini, 1954). The firing of many of the neurons in the hippocampal formation is paced by theta oscillations, suggesting that theta activity is important for the coordination of synaptic activity (Buzsaki, Leung, & Vanderwolf, 1983; Kramis, Vanderwolf, & Bland, 1975; L. W. Leung & Buzsaki, 1983). It has been linked to various computational processes such as memory formation, sensorimotor integration, and spatial navigation (Bland, 1986; Buzsaki, 2005; Cacucci, Lever, Wills, Burgess, & O'Keefe, 2004; Hasselmo, 2005), and it has been correlated with active navigational states in humans, such as maze-solving (Caplan et al., 2003). Synchronization of neuronal activity during theta activity is believed to play a critical role in regulating synaptic integration within the hippocampal formation by generating alternating states of depolarization and hyperpolarization. This can also impact on the induction of lasting changes in synaptic strength. For example, synaptic activation during the depolarizing or

hyperpolarizing phases of the theta rhythm can lead to lasting potentiation and depression of synaptic inputs, respectively (Buzsaki, 2002; Huerta & Lisman, 1993; Hyman, Wyble, Goyal, Rossi, & Hasselmo, 2003; Judge & Hasselmo, 2004). This may provide a mechanism for promoting synaptic changes related to learning and memory.

The EC and the hippocampus expresses robust theta activity in both *in vivo* and *in vitro* preparations that is generated by a number of network and cellular mechanisms (Alonso & Garcia-Austt, 1987a, 1987b; Alonso & Llinas, 1989; Bland, Colom, Konopacki, & Roth, 1988; L. W. Leung & Yim, 1991; Mitchell & Ranck, 1980). The superficial layers of the EC receive inputs from sensory cortices and project to the dentate gyrus and CA3 of the hippocampus, and these inputs may contribute to the synchronization of theta activity in the hippocampus (L. S. Leung, Roth, & Canning, 1995; L. S. Leung & Shen, 2004; Vanderwolf, Leung, & Cooley, 1985; Wu & Leung, 1998). Theta-frequency activity in the hippocampus is also mediated, in part, by cholinergic and γ-amino-butyric acid (GABA)-ergic inputs from the medial septum (Dickson, Trepel, & Bland, 1994). In addition to inputs from the septum, theta in the EC and hippocampus is also generated by membrane potential oscillations. When depolarized to near threshold levels by either depolarizing current or application of the cholinergic agonist, carbachol, oscillations in membrane potential occur in many cells of the hippocampus. The oscillations appear to be dependent on an interaction between a persistent sodium current (I_{Nap}) and a delayed potassium current (I_a), which is sufficient to generate theta-frequency membrane potential oscillations (Chapman & Lacaille, 1999a, 1999b; Dickson & Alonso, 1997; Klink & Alonso, 1993, 1997). Other reports show that voltage-dependent theta-frequency membrane potential oscillations in layer II

cells of the EC are the result of an interplay between the persistent sodium current (I_{Nap}) in the depolarizing direction, and the rhythmic and time-dependent activation and deactivation of the inward rectifying nonspecific cation current (I_h) (Dickson et al., 2000). Reactivation of this inward current by depolarization induces the hyperpolarizing phase of each oscillation. The resulting oscillations in individual neurons at near-threshold voltage levels may help generate theta-frequency population activities, and promote rhythmic depolarization that paces cell firing at theta-frequency (Engel, Fries, & Singer, 2001).

Although the PaS receives cholinergic inputs from the septum and is tightly linked to other structures in the hippocampal formation that display theta-frequency activity, whether theta-frequency EEG activity is generated locally by PaS cells is unknown. While cells that fire in relation to the phase of local theta activity have been previously reported in the PaS (Cacucci, Lever, Wills, Burgess, & O'Keefe, 2004; Taube, 1995b), and anatomical studies have reported extensive connections with brain structures associated with theta activity (Amaral & Witter, 1995; Caballero-Bleda & Witter, 1993, 1994; van Groen & Wyss, 1990b), theta activity has yet to be definitively localized to either the superficial or deep layers. The present studies have determined that theta-frequency EEG activity is generated locally within the superficial layers of the PaS in the urethane-anesthetized rat, and that it is dependent on activation of muscarinic cholinergic receptors. In order to determine whether the theta activity may be due in part to intrinsic membrane oscillations in superficial cells, whole-cell current clamp recordings in acute brain slices were used to record membrane potential in layer II cells of the PaS. Varying membrane potential with constant current injection was used to assess the voltage-

dependence of the membrane potential oscillations, and the role of synaptic inputs was assessed by pharmacological blockade of ionotropic glutamate and GABAergic receptors. Theta-frequency EEG activity was found to be generated locally in the superficial layers of the PaS, and intrinsic membrane potential oscillations are likely to contribute to the production of this activity.

METHODS

Recordings from Anesthetized Animals

Surgery. Data were obtained from seven male Long-Evans hooded rats (300 – 500g; Charles River, Montréal, Canada). Recording were also obtained from three additional rats that had electrodes pass either rostral or caudal to the PaS, however theta-frequency EEG activity was not observed in these cases (data not shown). The animals were anesthetized with an oxygen/isoflurane (98.5%/1.5% concentration) mixture in order to insert a cannula into the jugular vein. The rat was switched to anesthesia using urethane (0.8 g/ml, i.v.; Sigma, St. Louis, MO, USA), which allowed for the fine regulation of level of anesthesia for the remainder of the experimental procedures. A digital rectal thermometer was used to monitor body temperature, which was maintained at 36-37°C with a heating lamp throughout the experiment.

Animals were prepared for stereotaxic surgery in a standard manner. The rat was secured in a grounded Kopf stereotaxic apparatus (David Kopf Instr., Tujunga, CA) , and bregma and lambda were leveled. A stainless-steel jeweler's screw was placed in the right frontal bone as a reference electrode. A monopolar recording electrode made from Teflon-coated stainless-steel wire was placed in the CA1 region of the hippocampus (P, 4.5 mm; L, 3.0 mm relative to Bregma; and V, 2.1-2.7 mm from dural surface; Paxinos and Watson, 1998). The final depth was determined by maximizing the amplitude and clarity of theta-frequency activity (Bland, Anderson, & Ganes, 1975; Robinson, 1980). To obtain recordings from the PaS, a small opening was drilled in the side of the skull to allow the recording electrode to enter the brain at an angle of 30° above horizontal. Mineral oil was applied to the exposed dura. Differential recordings from a bipolar

electrode were used to minimize the impact of volume-conducted activity from the hippocampal formation on recordings of parasubicular EEG. The electrode was constructed from two insulated tungsten electrodes (10-50 μm tip diameter; FHC, Bowdoinham, ME) with one tip staggered 500-700 μm back from the other. The active, leading tip of the electrode was aimed at the surface of the PaS at a point 1.0 mm anterior from the interaural line, 3.8 mm from midline, and 5.0 mm above the interaural line (Caballero-Bleda & Witter, 1993; Paxinos & Watson, 1998). The bipolar recording electrode was aimed at this target and placed 2 mm away from target to begin recordings.

Depth profile recordings. Recordings were obtained from the bipolar electrode in 100 μm increments as it was moved along a 4 to 5 mm track using an oil-hydraulic manipulator (Narishige, MO-10). Each recording began with an initial five-second baseline period without theta activity in the hippocampus, followed by a tail-pinch to induce five-second period of theta-frequency EEG activity. Field activity was recorded simultaneously in the hippocampus and PaS, and was analog filtered (0.1 Hz to 10 kHz passband), amplified (x1000; A-M Systems, Model 1700), and monitored using a digital oscilloscope. Recordings were digitized at 20 kHz (12-bit) and recorded to hard disk using the software program Experimenter's Workbench (Datawave Technologies, Longhorn, CO).

Theta activity in the hippocampus and EC of urethane-anesthetized rats is dependent on cholinergic receptors, and is disrupted by the systemic administration of the non-selective muscarinic cholinergic antagonist atropine sulfate (Dickson, Trepel, & Bland, 1994; Kramis, Vanderwolf, & Bland, 1975). To determine if parasubicular theta is dependent on cholinergic inputs, atropine sulfate (Sigma; 10 mg/kg; (Natsume,

Hallworth, Szgatti, & Bland, 1999) was administered via the jugular cannula after the depth profile was completed. Recordings were obtained before and after atropine administration at the depth where maximal parasubicular theta was observed.

Histology. Upon completion of electrophysiological recordings, a cathodal current (100 μA for eight seconds) was passed through the leading tip of the parasubicular electrode to mark the tip locations at the depth of the PaS on the electrode track. The animal was then deeply anesthetized with urethane, and perfused transcardially with 0.9% saline followed by 10% formalin. Brains were stored in 10% formalin (Sigma), and transferred to a 30% sucrose solution three days before sectioning. Coronal sections (40 μm thick) were obtained and stained with cresyl violet (Sigma; 0.1%). Coronal sections containing hippocampal and parasubicular electrode tracks were photographed using a Sony XC-77 video camera, a Scion LG-3 frame grabber, and Image SXM (v1.6, S. D. Barrett, http://www.imageSXM.org.uk). Electrophysiological recordings were matched to locations on the recording track using the location of the target lesions. The thicknesses of cortical layers in the PaS were determined according to the convention of Amaral and Witter (1995) and Funahashi and Stewart (1997b).

Data processing. All signals were analyzed off-line using the software package, Origin 7.0 (OriginLab Corp., Northampton, MA). Two-second samples of EEG activity were selected at each depth along the recording electrode track to construct profiles of power of the locally-generated theta activity. Power profiles were constructed by calculating the total power between 3.1 and 10.4 Hz at each depth. The absolute amount of power in the EEG varied considerably across different animals, and theta-band power in depth profiles was therefore plotted as a proportion of maximal theta-band power for

each animal. The phase relationship between theta activity recorded in the superficial layers of the PaS and in the CA1 region was determined using cross-correlations of simultaneously recorded two second EEG samples and by the phase of the cross spectrum (Alonso & Garcia-Austt, 1987a). Because the phase of hippocampal theta depends on the laminar position of the CA1 electrode (L. W. Leung, 1984), which varied across different animals, the phase of the cross-spectrum was plotted as a function of the depth of the hippocampal electrode.

In vitro slice recordings

Methods were similar to those reported previously (Chapman & Lacaille, 1999b), and all chemicals were obtained from Sigma (St. Louis, MO).

Slice preparation. Acute brain slices were obtained from 4 to 6 week-old male Long-Evans rats (Charles River, Montréal, QC). The animal was anesthetized with halothane and decapitated. The brain was quickly removed from the skull, and submerged in cold (4°C) artificial cerebrospinal fluid (ACSF) containing (in mM): 124 NaCl, 5 KCl, 1.25 NaH_2PO_4, 2 $MgSO_4$, 2 $CaCl_2$, 26 $NaHCO_3$, and 10 dextrose saturated with 95% O_2 and 5% CO_2. To isolate the hippocampal formation, the cerebellum and frontal lobes were removed, and the brain was placed with the dorsal side adhered to a vibratome pedestal using methylmethacrylate adhesive. The brain was submerged in cold oxygenated ACSF, and horizontal brain slices (300 μm) were taken. Slices were allowed to recover for approximately one hour at room temperature, and individual slices were transferred to a recording chamber and visualized with an upright Leica DM-LFS light microscope (Leica Microsystems, Richmond Hill, ON) equipped with a differential interference contrast optics (COHU, San Diego, CA) and a long-range

water immersion objective (40x). Slices were superfused with oxygenated ACSF at room temperature at a rate of 1.5-3 ml/min. The location of layer II cells of the PaS was determined by using slice landmarks (ie. pial surface, angular bundle, and layer II of the medial EC and presubiculum), similar to protocols used by Funahashi and Stewart (1997b). The diffuse layer of disorganized cells that make up layer II of the PaS distinguish it from the compact layer II cells of the MEC and the presubiculum (Amaral & Witter, 1989; Funahashi & Stewart, 1997a, 1997b). Further, in contrast to deep layer parasubicular neurons, medial EC cells and subicular cells, none of the cells recorded here showed burst firing responses to current injection (Funahashi & Stewart, 1997a; R. S. Jones & Heinemann, 1988; Stewart & Wong, 1993).

Whole cell recordings. Patch pipettes were prepared from borosilicate glass (1.0mm OD, 5-10 MΩ) using a horizontal puller (Sutter Instruments, P-97, Novato, CA), and filled with a solution containing (in mM) 140 K-gluconate, 5 NaCl, 2 $MgCl_2$, 10 N-2-hydroxyethylpiperazine-N'-2-ethanesulfonic acid (HEPES), 0.5 ethylene glyco-bis (β-aminoethyl ether)-N,N,N',N'-tetraacetic acid (EGTA), 2 ATP-Tris, and 0.4 GTP-Tris. Electrodes were visually guided to contact the soma of layer II parasubicular neurons during the application of gentle positive pressure. Tight seals (>1 GΩ) were obtained using voltage-clamp with gentle suction, and increasingly strong suction was applied until whole cell configuration was established. Current clamp recordings were begun after a 3-5 min period to allow for the intracellular fluid and electrode solution to equilibrate. Membrane potential recordings (DC to10 kHz) were obtained with an Axoclamp 200B amplifier (Axon Instruments, Foster City, CA), visualized on a digital oscilloscope and digitized at 20 kHz (Axon Instruments, Digidata 1322A) for storage on

computer hard-disk using Clampex 8.1 software (Axon Instruments). Recordings were accepted if series resistance was <50 MΩ, displayed overshooting action potentials, and if the input resistance and resting membrane potential were stable. Series resistance was monitored repeatedly throughout recordings.

The ionic conductances responsible for the generation of membrane potential oscillations in the hippocampus and EC are voltage-dependent (Alonso & Klink, 1993; Alonso & Llinas, 1989; Chapman & Lacaille, 1999b; Dickson et al., 2000; Klink & Alonso, 1993). To determine if membrane potential oscillations in the superficial PaS are voltage-dependent, five to ten second duration recordings of membrane potential in the PaS were obtained at a range of voltages relative to the action potential threshold. The membrane potential was altered by varying the amount of steady current injection.

Recordings were obtained routinely at 22° C in order to reduce metabolic demands on the slices. However, to determine the frequency of MPOs in layer II cells of the PaS at more physiological temperatures, the temperature of the recording bath was increased to 32 ± 0.5 °C in 11 cells. Bath temperature was regulated using an automated temperature controller (Warner Instruments, Model TC-324B). Recordings at a range of voltages relative to action potential threshold were obtained at each temperature.

To determine whether membrane potential oscillations in layer II cells require synaptic input or are generated intrinsically, ionotropic glutamate receptors were blocked using 1,2,3,4-tetrahydro-6-nitro-2,3-dioxo-benzo(f)quinoxaline-7-sulfonamide disodium (NBQX, 10 μM) and (±)-2-amino-5-phosphonopentanoic acid (AP-5, 50 μM), and $GABA_A$ receptor-mediated synaptic transmission was blocked using bicuculline methiodide (BIC, 10 μM). After control tests in normal ACSF, recordings were obtained

at the same range of voltage levels after the application of pharmacological agents at either room temperature (n = 5) or 32° C (n = 6) to assess the contribution of synaptic inputs to the generation of membrane potential oscillations at both temperatures.

Data Analysis. Samples of membrane potential were prepared for spectral analysis by reducing the effective sampling rate to 1 kHz, and isolating 2.048 s segments of recording that contained no action potentials. The dominant frequency of the membrane potential oscillations was calculated by computing the power spectra after passing samples through a Blackman window (Clampfit 8.2, Axon Instruments). Cells that failed to show a clear peak in the power spectrum were considered to be non-oscillatory. Changes in the peak frequency of oscillations after drug application or temperature manipulations were assessed using matched samples t-tests.

Electrophysiological characteristics of layer II parasubicular cells were analyzed using the software program Clampfit 8.2 (Axon). Action potential height was measured from resting membrane potential and action potential width was measured from action potential threshold. Fast and medium afterhyperpolarizations were measured from action potential threshold. Input resistance was calculated by measuring the peak voltage response to a –200 pA current step (300 ms). Inward rectification was quantified by expressing the peak input resistance as a proportion of the steady-state resistance measured at the end of the negative current pulse (rectification ratio) (Chapman & Lacaille, 1999b). Data were expressed as mean ± SEM.

RESULTS

Theta Activity in the Anesthetized Animal

Differential recordings from bipolar electrodes were used to localize theta activity in the PaS of 7 urethane-anesthetized adult male rats. Monopolar recordings from the individual tips of the bipolar electrode contained large-amplitude theta activity along the entire electrode track that was phase-locked to theta activity in the CA1 region. Because these monopolar recordings largely reflect volume conduction from the hippocampus, only data from bipolar recordings are shown here. In 3 cases when the bipolar electrode passed either rostral or caudal to the PaS, there was no theta-frequency activity recorded (data not shown). Histological analysis revealed that, in cases in which theta-frequency activity was recorded from the bipolar electrode, the electrodes passed through the PaS (Figure 2B).

In all 7 animals, theta activity elicited by tail-pinch was observed in the CA1 region of the hippocampus. Local generation of theta activity in layer II of the EC is associated with a distinct phase-reversal of theta activity in the superficial and the deep layers (Alonso & Garcia-Austt, 1987a). To localize the layers in which theta activity is generated in the PaS, samples of field potential were recorded along a 4 mm track, starting 2 mm from the surface of the PaS. No theta activity was observed at sites near the beginning of the electrode track in the differential recordings, but theta-frequency oscillations were observed transiently as the bipolar electrode spanned the superficial layers of the PaS (Figure 2A, B). A phase-reversal between the superficial and deep layers results in negative recordings in superficial layers when the polarity is positive in deep layers, and opposite polarities at each tip of the electrode greatly enhances

differential recordings. After the bipolar electrode passed through the PaS, the amplitude of theta activity in the differential recording electrode was reduced, while theta-frequency activity in the stationary hippocampal electrode was maintained in response to tail-pinch (Figure 5C).

To quantify differences in the power of theta-frequency EEG activity (4-12 Hz; Bland, 1986) along the entire electrode track, power spectral analysis of representative traces was conducted at each depth. In order to compare depth profiles across animals, total theta-frequency power in the band from 3.1 to 10.4 Hz was expressed as a percentage of the maximal theta-band power observed along the electrode track. Both hippocampal and PaS recordings demonstrated clear peaks in the power spectrum corresponding to low-end theta frequencies (~3-6 Hz), and this is consistent with the frequency range of theta both the hippocampus and EC in the urethane-anesthetized rat (Bland, 1986; Dickson, Trepel, & Bland, 1994). The maximal amount of theta-band power was always observed as the electrode passed through the superficial layers of the PaS (Figure 2C). Due, in part, to variation in electrode tip separation, which ranged from 500 μm to 700 μm, maximal theta-band power varied across animals, which ranged from 0.004 to 0.016 mV, and had a mean of 0.007 ± 0.002 mV (n = 7). In each case, maximal theta-band power values were observed when the leading electrode tip was located 100-250 μm from the surface of the cortex (Figure 2C). Histological analysis revealed that this corresponded to electrode locations in layers II/III of the PaS, with the deep tip located in the deep layers of the PaS.

Cross-correlational analyses

Cross-correlational analyses were used to investigate the phase relationship between parasubicular and hippocampal theta-frequency EEG activity. The phase of hippocampal theta-frequency activity is known to vary systematically with depth across the lamina of the CA1 region (L. W. Leung, 1984). Accordingly, we found that the phase relationship between hippocampal and parasubicular theta activity is dependent on the exact location of the hippocampal reference electrode. Specifically, when the hippocampal electrode was placed in the stratum oriens, theta-frequency activity recorded in the PaS tended to be out of phase, while it was more phase-locked when the hippocampal electrode was positioned deep in the stratum radiatum (e. g., Figure 3A, B). In 4 animals in which the hippocampal electrode was located in the stratum radiatum and lacunosum-moleculare region of the CA1 region of the hippocampus, the average phase delay was only –17° (-47°, -39°, 35°, and –18°, respectively). Conversely, in the remaining 3 animals, when the reference electrode was placed near the stratum oriens, the average phase of PaS theta was more reversed in phase at 207° (-220°, 289°, and 113°, respectively) [t (5) = 4.67, $p < 0.01$] (Figure 3C).

Cholinergic dependence of parasubicular theta oscillations

Theta-frequency activity in the hippocampus of the urethane-anesthetized rat is paced by GABA-ergic and cholinergic neurons in the medial septum (Bland, 1986; Bland & Oddie, 2001; Denham & Borisyuk, 2000; Sotty et al., 2003; Vertes & Kocsis, 1997) and can be blocked by systemic administration of cholinergic antagonists. The non-specific muscarinic cholinergic antagonist, atropine sulfate, abolishes theta-frequency field oscillations in the hippocampal formation (Kramis, Vanderwolf, & Bland, 1975)

(Figure 4A). Similarly, systemic administration of atropine blocked theta-frequency activity elicited by tail-pinch in both the CA1 and PaS. Theta-frequency activity, as a percent of total power was reduced from 45.0 ± 5.6 % to 15.7 ± 3.3 % in the CA1 [t (3) = 3.79, $p < 0.01$] and from 51.8 ± 2.4% to 15.5 ± 5.0 % [t (3) = 10.10, $p < 0.01$] in the PaS (Figure 4B). Muscarinic antagonists therefore greatly reduce theta-frequency EEG activity in the PaS.

Theta-frequency membrane potential oscillations in layer II of the PaS

Whole-cell current clamp recordings were obtained from 21 layer II PaS cells. The basic electrophysiological characteristics of 17 parasubicular cells demonstrated electrical properties similar to the stellate and pyramidal cells described previously (Funahashi & Stewart, 1997a) (Figure 5B). Four cells demonstrated electrophysiological properties characteristic of interneurons, and were therefore analyzed separately (see below; Chapman & Lacaille, 1999b; Lacaille & Schwartzkroin, 1988).

The superficial layers of the PaS contain both stellate and pyramidal neuron cell types, however they display similar electrophysiological characteristics and thus were analyzed as a single set of data (Funahashi & Stewart, 1997a). Cells had a mean resting potential of -55.31 ± 1.93 mV upon initial whole-cell configuration, and a moderate input resistance (114.0 ± 9.7 MΩ). All 17 cells demonstrated some delayed inward rectification in response to hyperpolarizing current steps (mean of rectification ratio: 1.17 ± 0.03; range: 1.06 to 1.46) (Funahashi & Stewart, 1997a). Action potentials (amplitude: 101.67 ± 2.81 mV; width: 1.30 ± 0.06 ms) were typically followed by a fast and medium afterhyperpolarizations (fAHP amplitude: 7.46 ± 0.50 mV; mAHP amplitude: 6.12 ± 0.41

mV). Cells in the superficial layers of the PaS displayed high action potential threshold values (mean: -46.35 ± 1.47 mV).

Intrinsic voltage-dependent oscillations

In normal ACSF at 22° C, PaS cells did not usually fire at rest. However, upon steady positive current injection to threshold voltages (typically <50 pA), the majority of cells (14 out of 17 cells or 82.3%) displayed oscillations at frequencies between 2 and 5 Hz. When the cells were depolarized to suprathreshold voltage levels, the oscillations persisted between single spikes (Figure 5A). The cells did not, however, demonstrate cluster firing at consecutive peaks of the oscillations, as has been reported previously in hippocampal interneurons (Chapman & Lacaille, 1999b). The oscillations were markedly voltage-sensitive, and hyperpolarization of cells to 6-12 mV below threshold abolished oscillations.

A subset of the cells was further analyzed in detail for voltage-dependence of the oscillations. The power of oscillations increased significantly when membrane potential was increased from 6 mV below threshold (mean: 0.032 ± 0.007 mV^2/Hz) to threshold levels (mean: 0.111 ± 0.021 mV^2/Hz) [t (5) = 3.35, $p < 0.01$] (Figure 5C). Similarly, the peak-to-peak amplitude of oscillations also increased from 1.12 ± 0.09 mV to 2.40 ± 0.36 mV [t (5) = 3.32, $p < 0.01$] when membrane potential was increased to near threshold levels. The frequency of the oscillations was reflected by clear peaks in the power spectrum (Figure 5C). Oscillation frequency increased from 2.85 ± 0.26 Hz at 6 mV below threshold to 3.81 ± 0.24 Hz when the membrane potential was increased to near threshold voltages [t (5) = 2.58, $p < 0.05$].

The frequency of membrane potential oscillations increased to within the range of frequencies of endogenous theta-frequency activity (4 –12 Hz) at more physiological temperatures (Bland, 1986; Chapman & Lacaille, 1999b; Petsche, Stumpf, & Gogolak, 1962). Bath temperature was increased to 32° C to determine if the frequency of membrane potential oscillations in layer II cells of the PaS was temperature-sensitive. Recordings at all voltage-levels were repeated when the temperature of the bath was increased from 22° C to 32° C (n = 11). Numerous electrophysiological characteristics of the PaS cells were altered at increased temperatures, consistent with increased K^+ kinetics associated with whole-cell recordings at physiological temperatures (Shen & Schwartzkroin, 1988; Thompson, Masukawa, & Prince, 1985). At the increased temperature, the cells displayed a decrease in spike amplitude (100.52 ± 5.50 mV at 32° C vs. 108.51 ± 3.88 mV at 22° C), and a decrease in the input resistance (72.90 ± 7.60 MΩ vs. 122.10 ± 10.09 MΩ) (Figure 6B). A smaller sample of cells was selected for power spectrum analysis (n = 9). Raising the temperature of the bath from 22° C to 32° C increased the frequency [3.44 ± 0.22 Hz to 5.96 ± 0.32 Hz; t (8) = 7.44, $p < 0.001$] (Figure 6A, D), but did not affect the power of the oscillations (0.055 ± 0.009 at 22° C Vs. 0.065 ± 0.016 at 32° C; $p > 0.05$) (Figure 6C).

Receptor blockers were used to determine whether oscillations are intrinsic, or may be due to extrinsic glutamatergic or GABAergic synaptic inputs. Recordings were repeated in normal ACSF and during bath application of the *N*-methyl-*D*-aspartate (NMDA) glutamate receptor blocker DL-(±)-2-amino-5-phosphonopentanoic acid (AP-5; 50 μm), non-NMDA receptor blocker 1,2,3,4-tetrahydro-6-nitro-2,3-dioxo-benzo[f]quinoxaline-7-sulfonamide disodium (NBQX; 10 μm), and $GABA_A$ receptor

blocker bicuculline (BIC; 20 μm) ($n = 4$) (Figure 7A). The peak frequency and power of membrane potential oscillations were not significantly altered during application of receptor blockers (3.54 ± 0.35 Hz in ACSF vs. 4.39 ± 0.65 Hz in antagonists, $p > 0.05$; 0.078 ± 0.020 mV^2/Hz in ACSF vs. 0.061 ± 0.031 mV^2/Hz in antagonists, $p > 0.05$), indicating that generation of membrane potential oscillations in layer II cells of the PaS does not require extrinsic ionotropic glutamate or $GABA_A$ synaptic input (Figure 7C, D).

Increasing the temperature of the bath increases the frequency of membrane potential oscillations, but also increases the level of synaptic activity in the acute slice. To determine whether augmented synaptic activity at 32° C contributed to increases in the frequency of oscillations, recordings at 32° C were repeated in some cells during bath application of ionotropic glutamatergic and GABAergic antagonists NBQX, AP-5, and bicuculline ($n = 4$). The oscillations were not reduced in frequency or power (6.47 ± 0.64 Hz in ACSF vs. 7.81± 1.11 Hz in antagonists, $p > 0.05$; 0.036 ± 0.017 in ACSF vs. 0.042 ± 0.012, $p > 0.05$), suggesting that membrane potential oscillations in layer II cells at 32° C are regulated largely by intrinsic conductances rather than synaptic input (Figure 7D).

Interneurons in the PaS

Inhibitory interneurons have been identified previously in the PaS using parvalbumin staining (van Vliet, Aronica, Tolner, Lopes da Silva, & Gorter, 2004). A small group of cells ($n = 4$) demonstrated electrophysiological characteristics similar interneurons in other areas of the hippocampal formation (Chapman & Lacaille, 1999a). Cells were differentiated from other PaS cells by their high input resistance [mean: 264.25 ± 48.94 MΩ; t (3.239) = 3.01, $p < 0.05$], short action potential duration (mean: 1.12 ± 0.13 ms), and a large fAHP amplitude [mean: 13.45 ± 2.01 mV; t (19) = 3.75, $p <$

0.05]. These cells had a mean resting membrane potential of -57.02 ± 2.54 mV. Three of the 4 cells showed a large delayed inward rectification, however this did not significantly differ from other parasubicular cells (Figure 8B; interneurons: 1.49 ± 0.35 vs. other PaS cells: 1.17 ± 0.03, $p > 0.05$).

Of particular interest is the observation of voltage-dependent theta-frequency membrane potential oscillations in these cells. Inhibitory interneurons in the hippocampal formation can demonstrate intrinsic membrane potential oscillations, which may serve to rhythmically inhibit or disinhibit principal cells, and may serve to synchronize neural networks into either theta or gamma frequencies (Chapman & Lacaille, 1999b). When depolarized to near-threshold levels, the membrane potentials of the four putative interneurons oscillated at a mean frequency of 3.88 ± 0.58 Hz, and this increased to 6.49 ± 0.42 Hz at 32° C (Figure 8A, C), without significant reductions in power (Figure 8C) [$n = 3$; $t\,(2) = 6.21$, $p < 0.05$). Similar to other PaS cells, oscillations were abolished when membrane potential was hyperpolarized (Figure 8A). Finally, oscillations in these interneurons were found to be independent of fast ionotropic synaptic transmission, and persisted in the presence of NBQX, AP5 and bicuculline ($n = 1$, data not shown).

Figure 1. A summary diagram detailing the extrinsic cortical and subcortical connections with the parasubiculum. Bold lines indicate major projections. The CA1 region of the hippocampus and the medial septum send major projections to the superficial layers of the parasubiculum, which in turn sends a major projection exclusively to the superficial layers of the entorhinal cortex (adapted from Amaral & Witter, 1995).

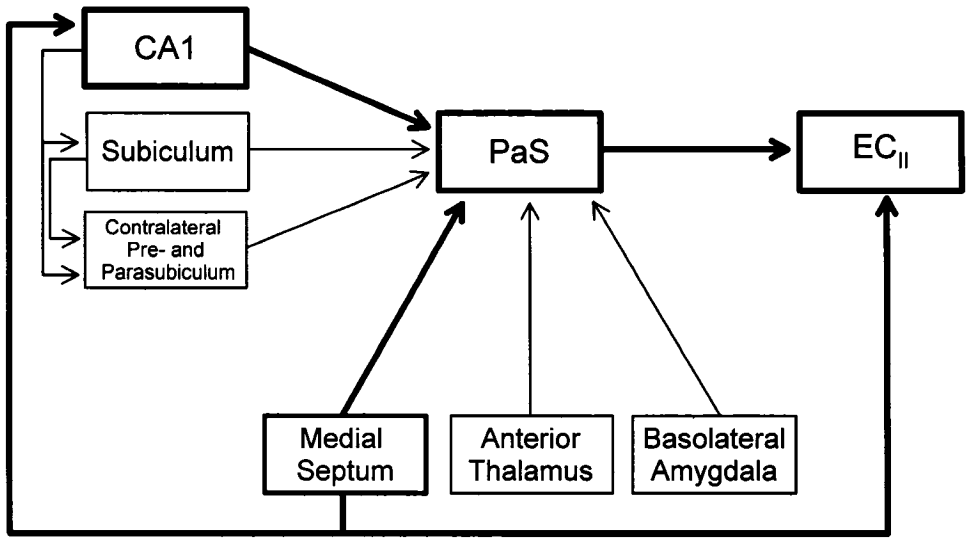
CA1
Subiculum
Contralateral Pre- and Parasubiculum
PaS
EC$_{II}$
Medial Septum
Anterior Thalamus
Basolateral Amygdala

Figure 2. Theta-frequency EEG activity is generated locally within the superficial layers of the parasubiculum. **A.** Differentially recorded EEG activity from a bipolar electrode that passed through the parasubiculum is shown with simultaneous recordings from a stationary reference electrode in the CA1 region of the hippocampus. The locations at which recordings were obtained are indicated by numbers that correspond to the locations in B_1. Note that theta-frequency EEG activity was observed only in traces obtained from positions 2 to 4 as the leading tip of the electrode passed through layers I and II of the PaS. Theta activity elicited by tail-pinch was observed in the CA1 region during each of these recordings. **B.** Locations from which recordings in A were obtained are shown in a photomicrograph (B_1). Recording electrode tracks are shown for all 7 animals in B_2. The dashed line in B_2 indicates the trajectory of the track shown in B_1. The shaded area indicates the location of the PaS. **C.** Depth profiles for each of the 7 animals tested show changes in the amount of theta-band power as the bipolar recording electrode was passed through the parasubiculum. Data for the 7 animals tested are shown on separate panels for clarity, and data are expressed as a proportion of the maximal theta-band power observed along the electrode track. Maximal theta-band power was observed within 0.1 to 0.3 mm of the surface of the cortex in layers I to II of the parasubiculum.

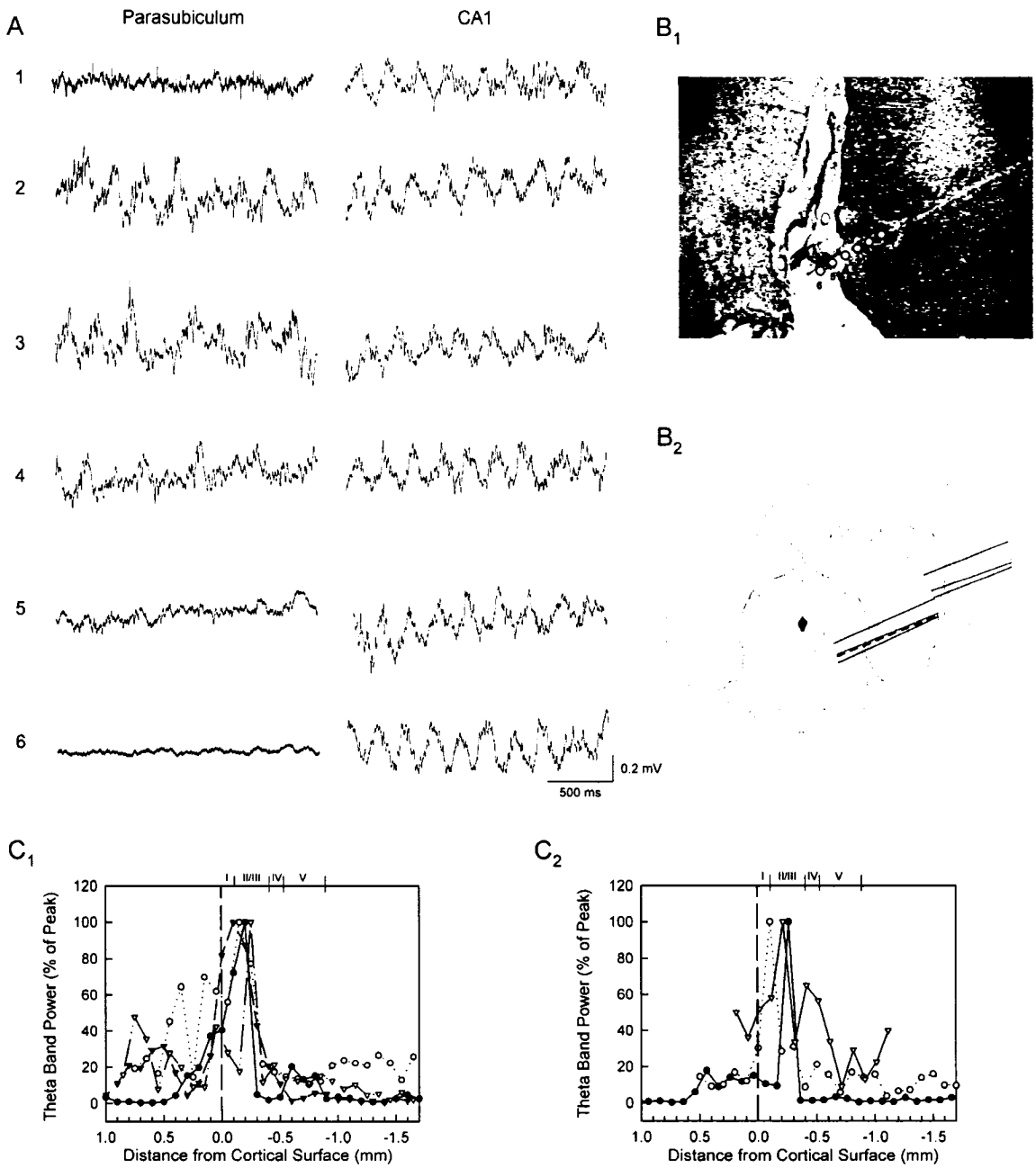
A
Parasubiculum
CA1
1
2
3
4
5
6
0.2 mV
500 ms
B1
B2
C1
C2
Theta Band Power (% of Peak)
Distance from Cortical Surface (mm)
I
II/III
IV
V
120
100
80
60
40
20
0
1.0
0.5
0.0
-0.5
-1.0
-1.5

Figure 3. Theta activity in the parasubiculum is phase-locked to simultaneously recorded theta activity in stratum radiatum of the CA1 region. **A.** Samples of simultaneously recorded EEG activity in the CA1 region and in the parasubiculum. **B.** The cross correlation of records in A reflects strong theta activity shared in both sites. The peak in the cross correlation close to a lag of zero (arrow) indicates the signals were nearly phase-locked. **C.** The phase of the cross correlation functions in different animals depended on the laminar location of the reference electrode in the CA1 region. Parasubicular theta was near phase-locked to theta activity recorded in stratum radiatum, and was more phase reversed relative to theta activity recorded in stratum oriens. The open circle indicates the phase relation obtained for the recordings in A.

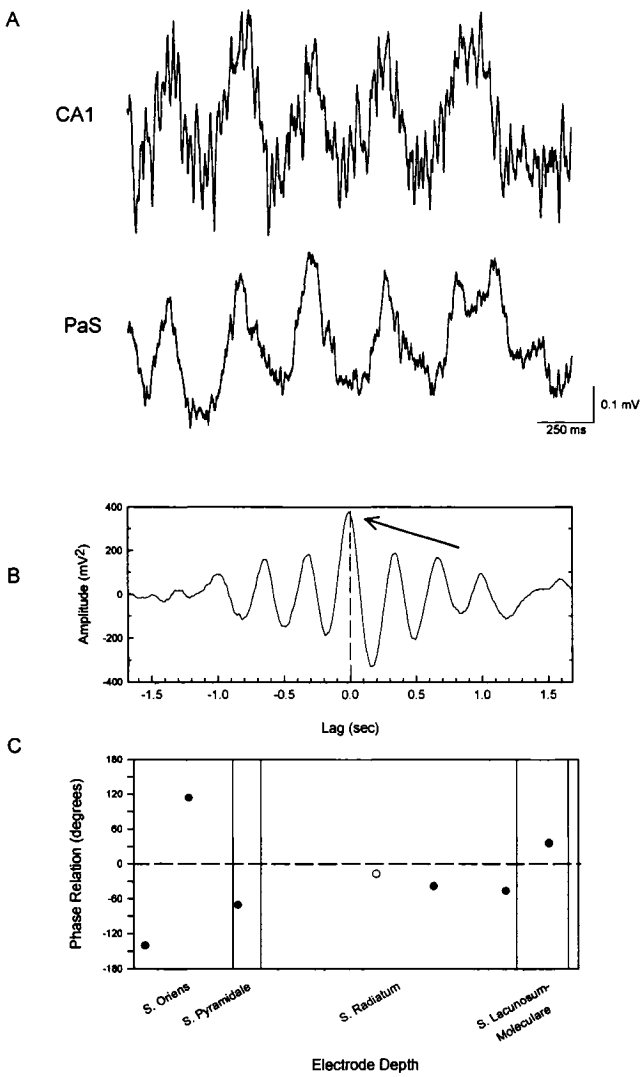
A
CA1
PaS
0.1 mV
250 ms
B
Amplitude (mV2)
400
200
0
-200
-400
-1.5
-1.0
-0.5
0.0
0.5
1.0
1.5
Lag (sec)
C
Phase Relation (degrees)
180
120
60
0
-60
-120
-180
S. Oriens
S. Pyramidale
S. Radiatum
S. Lacunosum-Moleculare
Electrode Depth

Figure 4. Blockade of muscarinic cholinergic receptors abolishes theta-frequency EEG activity in both the parasubiculum and the CA1 region. **A.** Representative simultaneous recordings are shown for each site before (A_1) and after (A_2) systemic administration of 10 mg/kg atropine sulfate. **B.** Group averages of theta-band power show significant reductions following atropine in both recording sites (*, $p < 0.01$).

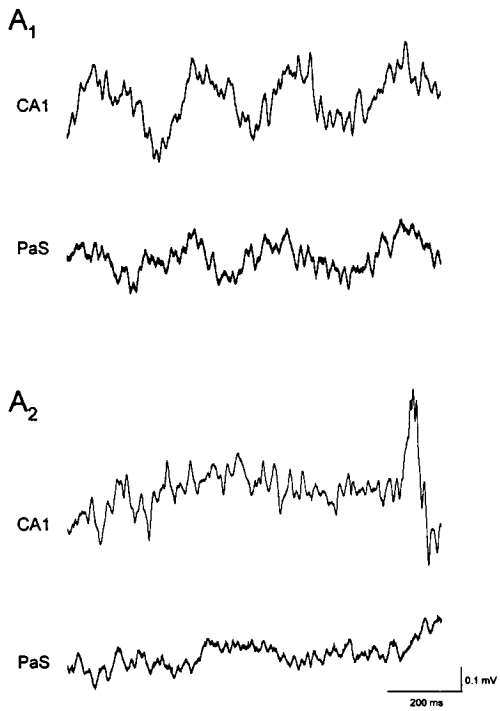
A1
CA1
PaS
A2
CA1
PaS
0.1 mV
200 ms
B
Baseline
Atropine
Theta-band Power (% of total)
80
60
40
20
0
*
*
CA1
PaS

Figure 5. Neurons in layer II of the PaS display voltage-sensitive oscillations in membrane potential. **A.** Whole-cell current clamp recordings from a representative parasubicular neuron are shown at the membrane potentials indicated at left. When the cell was held near threshold by positive current injection membrane potential oscillations occurred at a frequency near 4 Hz and contributed to the timing of action potentials. Action potentials are truncated in this and subsequent figures. Oscillations were not observed at more hyperpolarized potentials. **B.** Membrane potential responses to hyperpolarizing and depolarizing current pulses delivered at resting potential in normal ACSF in the same cell as in A. Note the moderate delayed inward rectification during strong hyperpolarizing pulses. Action potentials are truncated. **C.** Power spectra for recordings obtained at three voltage levels from the same cell as in A and reflect a peak frequency of oscillations between 2 and 5 Hz, and a shift to higher frequencies at depolarized membrane potentials (C_1). The power of oscillations are shown as a function of membrane potential relative to spike threshold for a sample of 7 neurons in C_2. Note the increasing power of oscillations as membrane potential was increased to near-threshold levels.

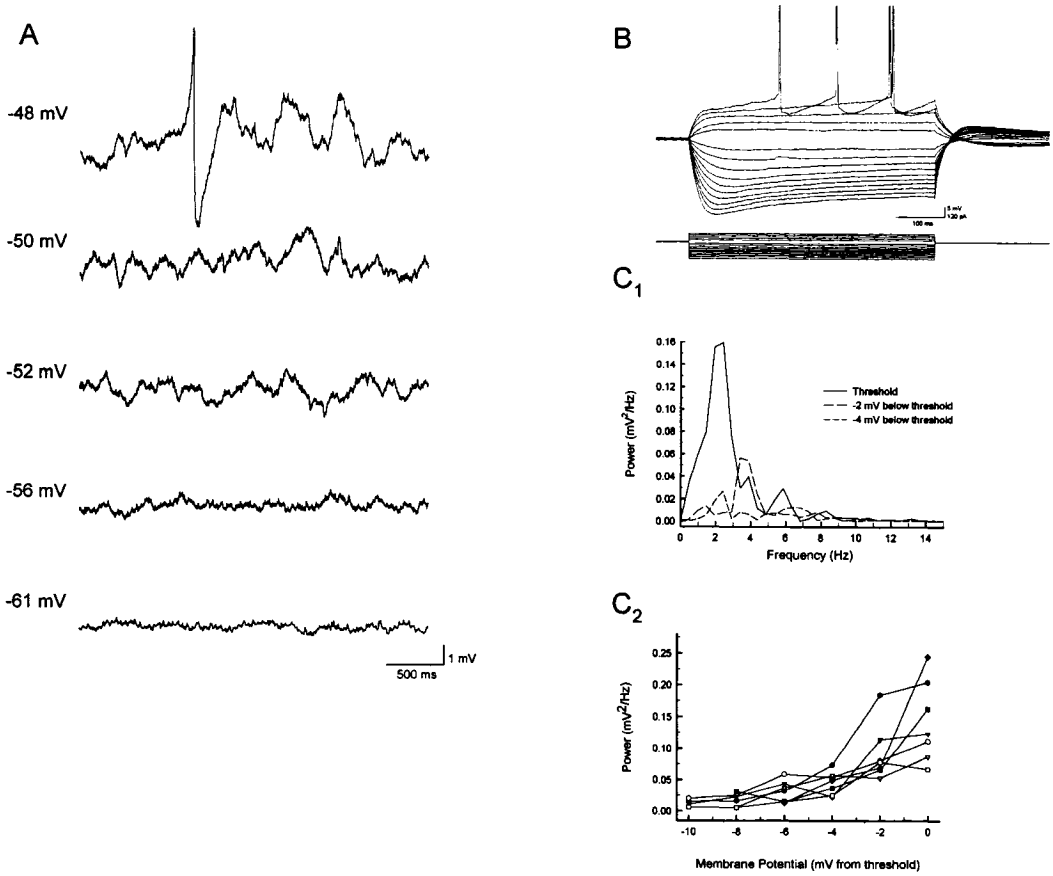
A
-48 mV
-50 mV
-52 mV
-56 mV
-61 mV
1 mV
500 ms
B
C1
Power (mV²/Hz)
Threshold
-2 mV below threshold
-4 mV below threshold
Frequency (Hz)
C2
Power (mV²/Hz)
Membrane Potential (mV from threshold)

Figure 6. The frequency of oscillations increased when the temperature of ACSF was raised from 22° to 32° C. **A.** Recordings from a representative neuron at the indicated voltages at 22° and 32° C. Note that oscillations at both temperatures are abolished by hyperpolarization. **B.** Membrane potential responses to current steps in the same neuron as in A at 22° C show moderate inward rectification. **C.** Comparison of power spectra of membrane potential at voltage levels just below spike threshold are compared for recordings from the same cell at 22° and 32° C. Note the increase in peak frequency of oscillations with little change in power of oscillations. Initial peaks in both spectra at frequencies near 1.0 Hz reflect slower, non-oscillatory changes in membrane potential. **D.** There was a significant increase in the peak frequency of oscillations in the group of cells tested (n= 11; $p < 0.05$).

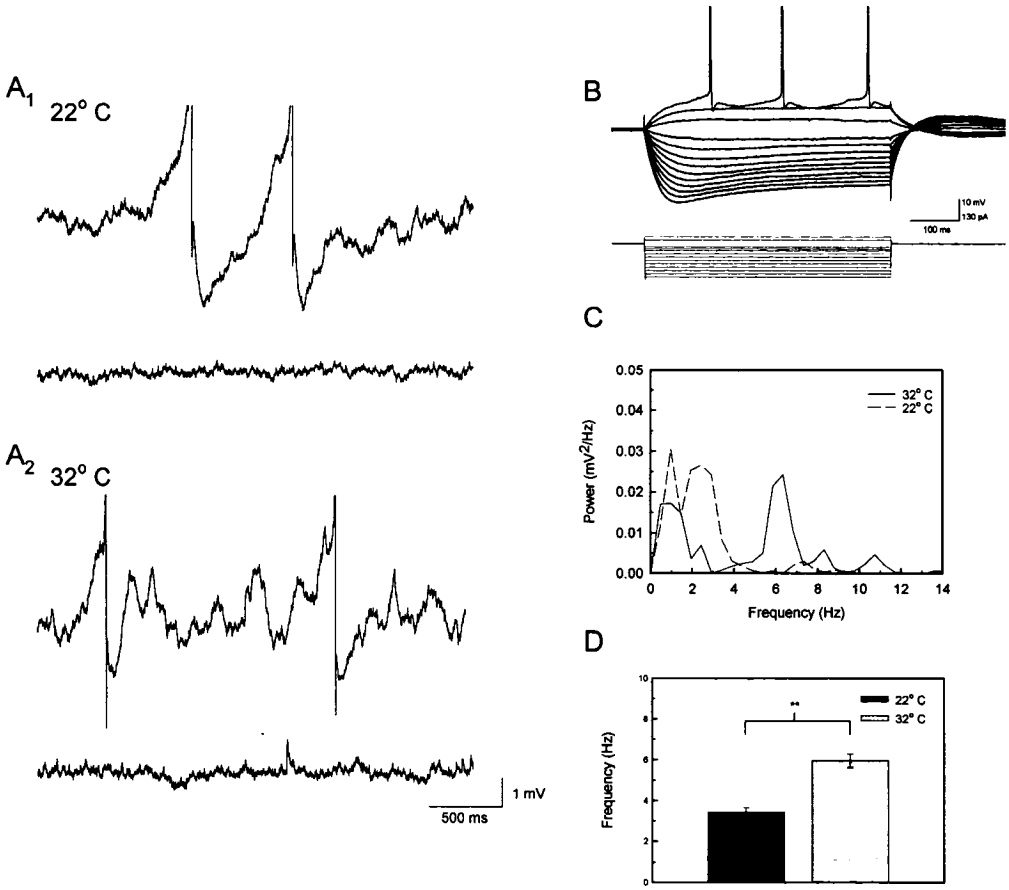
A1
22° C
A2
32° C
1 mV
500 ms
B
10 mV
130 pA
100 ms
C
32° C
22° C
Power (mV²/Hz)
0.05
0.04
0.03
0.02
0.01
0.00
0
2
4
6
8
10
12
14
Frequency (Hz)
D
22° C
32° C
**
Frequency (Hz)
10
8
6
4
2
0

Figure 7. Membrane potential oscillations persist in the presence of blockers of ionotripic glutamate- and GABA-mediated synaptic transmission. **A.** Recordings from a layer II parasubicular neuron at the indicated voltage levels are shown for before (A_1) and after (A_2) blockade of ionotropic glutamatergic and GABAergic synaptic transmission with NBQX (10 μM), AP-5 (50 μM), and bicuculline (10 μM). Recordings were conducted at 22° C. **B.** Membrane potential responses to current steps in the same neuron as in A. **C.** Power spectra of traces in A recorded at –47 mV show no change in power or frequency of membrane potential oscillations in the presence of synaptic blockers. **D.** Group averages of neurons recorded at 22° C ($n = 4$) and 32° C ($n = 4$) show that blockade of synaptic transmission has no significant effect on frequency of oscillations at either temperature ($p = 0.49$). The persistence of voltage dependent oscillations during the blockade of ionotropic synaptic transmission suggests that oscillations are generated by intrinsic conductances.

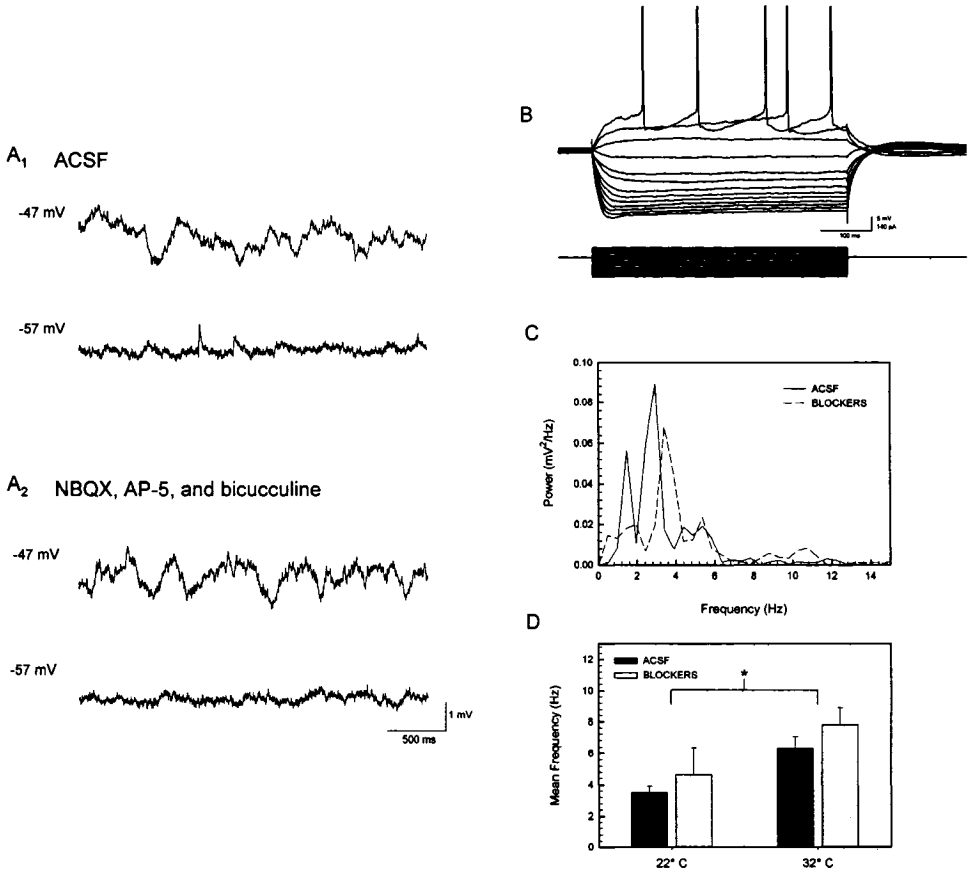
A1 ACSF
-47 mV
-57 mV
A2 NBQX, AP-5, and bicucculine
-47 mV
-57 mV
1 mV
500 ms
B
C
ACSF
BLOCKERS
Power (mV²/Hz)
Frequency (Hz)
D
ACSF
BLOCKERS
*
Mean Frequency (Hz)
22° C
32° C

Figure 8. Putative inhibitory interneurons in layer II of the PaS also display temperature- and voltage-dependent membrane potential oscillations. **A.** Representative recordings from one of the four interneurons displays voltage-sensitive membrane potential oscillations at both 22° (A_1) and 32° C (A_2) which are abolished by hyperpolarization from threshold. **B.** Voltage responses to hyperpolarizing current steps reflect a high input resistance (353 MΩ). Note the marked sag in the voltage response to large hyperpolarizing current pulses. Putative interneurons also has short spike widths and large fast afterhyperpolarizations. **C.** Power spectra of traces recorded from the neuron in A show an increase in the peak frequency of oscillations as temperature was increased from 22° to 32° C. Note the temperature-dependent increase in the peak frequency of oscillations that is similar to the increased frequency of oscillations observed at 32° C in principal neurons.

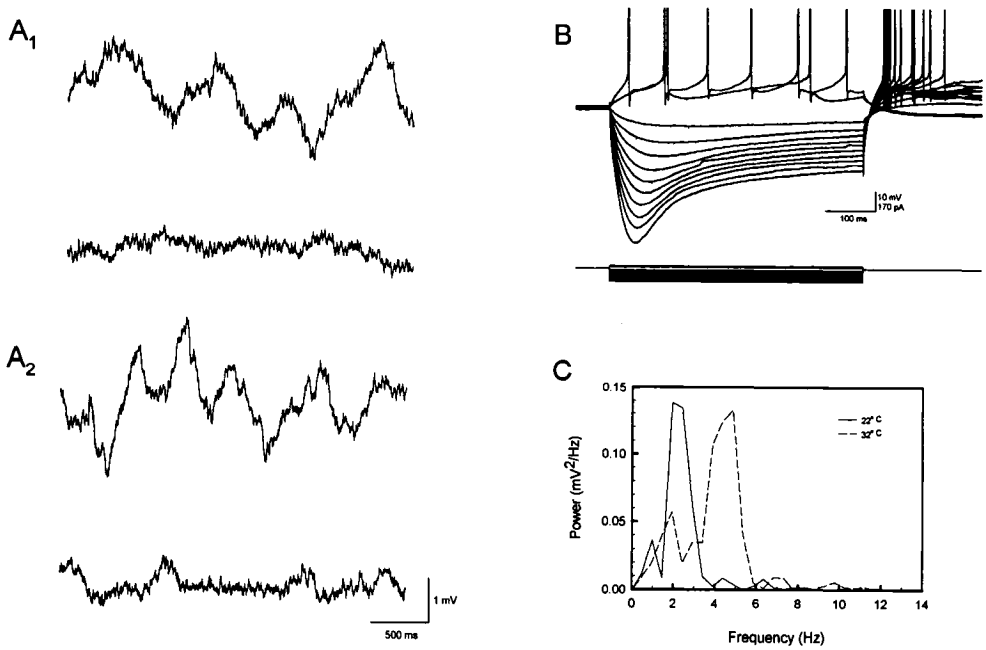
A1
A2
1 mV
500 ms
B
10 mV
170 pA
100 ms
C
22° C
32° C
Power (mV²/Hz)
0.15
0.10
0.05
0.00
0
2
4
6
8
10
12
14
Frequency (Hz)

DISCUSSION

The local generation of theta-frequency EEG activity within the PaS has been demonstrated here using both *in vivo* and *in vitro* electrophysiological techniques. Both theta activity and the PaS are known to play important roles in spatial navigation, the integration of sensory information, and mnemonic processes (Bland & Oddie, 2001; Buzsaki, 2005; Cacucci, Lever, Wills, Burgess, & O'Keefe, 2004; Caruana & Chapman, 2004; Hasselmo, 2005; Vertes, 2005). While cells in the PaS that fire with constant phase relationships to theta-frequency activity have been recorded, and local theta field activity in the PaS has been reported previously in freely moving animals (Cacucci, Lever, Wills, Burgess, & O'Keefe, 2004; Taube, 1995b), this is the first definitive demonstration of the local generation of theta-frequency field activity in the superficial layers of the PaS. Bipolar electrodes were used in the urethane-anesthetized rat to detect theta-frequency activity that was phase reversed across the superficial layers, rather than theta activity that is passively volume-conducted from the hippocampus that shows no phase reversal. Tail-pinch stimulation elicited theta-frequency activity both in the hippocampus and in the superficial layers of the PaS. Similar to theta-frequency activity other structures in the hippocampal formation (Kramis, Vanderwolf, & Bland, 1975; Vanderwolf, 1969), theta field activity in the PaS was blocked by atropine, and is therefore dependent on muscarinic receptor activation. The major output of layer II of the PaS is to layer II of the EC (Amaral & Witter, 1989, 1995; Caballero-Bleda & Witter, 1994; Swanson & Cowan, 1979; van Groen & Wyss, 1990b), and the present finding suggests that this output may play an important role in modulating sensory processing in the EC during theta activity (Caruana & Chapman, 2004).

Intrinsic membrane potential oscillations are known to contribute to the generation of theta-frequency activity in various regions of the hippocampal formation and adjacent structures, such as the basolateral amygdala (Alonso & Llinas, 1989; Bland, Konopacki, & Dyck, 2002; Bonansco & Buno, 2003; Chapman & Lacaille, 1999b; Pape, Pare, & Driesang, 1998). Using visually guided whole-cell current clamp recordings, we have found that layer II cells of the PaS also demonstrate voltage-dependent oscillations in membrane potential at theta-frequency. These oscillations persist during blockade of fast glutamate- and $GABA_A$-mediated synaptic transmission, suggesting that they are generated intrinsically. Similarly, the frequency of the oscillations increased to within the frequency range of theta activity observed *in vivo* at more physiological temperatures. This suggests that intrinsically generated membrane potential oscillations may contribute to the production of theta-frequency EEG activity *in vivo*.

The present studies provide the first evidence of the local generation of theta-frequency oscillations in the superficial layers of the PaS, and furthermore suggest that they are mediated in part by intrinsic membrane potential oscillations. This is consistent with previous reports of theta-related activity in the PaS. Taube (1995b) reported that 41% of parasubicular cells fire in relation to theta activity. Similarly, Cacucci and colleagues (2004) reported local theta-frequency EEG activity in both the presubiculum and the PaS. These authors used tetrodes to differentially record local field activity, however and the placement of the reference electrode was not described. These studies were therefore not able to definitively localize the origin of the theta-frequency activity. Using differential bipolar electrodes to eliminate volume-conducted activity from adjacent hippocampal structures, and recording at an angle perpendicular to the laminar

orientation of the PaS, we were able to localize the generation of theta-frequency activity to the superficial layers of the PaS.

Local generation of theta-frequency activity in the PaS. The local generation of hippocampal theta activity *in vivo* has been previously evidenced by the reversal of the polarity of oscillations relative to a stationary electrode when the active electrode passes through the cell layers that generate theta activity. There are two main generators located in the CA1 region and in the dentate gyrus, and they both contribute to a shift in the phase of theta activity within the hippocampal formation (Alonso & Garcia-Austt, 1987a; Bland, Anderson, & Ganes, 1975). Specifically, there is a gradual phase shift throughout the CA1 region of the hippocampus starting from the stratum oriens to stratum lacunosum moleculare. Compared theta activity recorded in stratum oriens, theta activity in the stratum lacunosum-moleculare and stratum radiatum is roughly 130-160° out of phase (Bland, Anderson, & Ganes, 1975; Kowalczyk & Konopacki, 2002; L. W. Leung, 1984). This pattern can be accounted for by the presence of two competing voltage dipoles generated by the interaction of rhythmic somatic inhibition of pyramidal cells in stratum oriens/pyramidale and synaptic currents in the apical dendrites of the stratum radiatum (Buzsaki, 2002).

Layer II of the EC also generates theta activity, and there is a reversal in the phase of theta-frequency EEG in the EC between the superficial and deep layers (Alonso & Garcia-Austt, 1987a; Mitchell & Ranck, 1980). Layer II cells of the EC projects almost exclusively to the dentate gyrus via the perforant path, and the cells of the dentate gyrus, in turn, contribute to the rhythmic, synchronized firing of CA1 pyramidal cells (Amaral & Witter, 1989, 1995; L. S. Leung, Roth, & Canning, 1995; Wu & Leung, 1998). Since

the PaS exclusively sends efferents to layer II of the EC, it is possible that the PaS may help pace or generate theta-frequency EEG activity in the EC.

Early pilot studies using monopolar electrodes showed that theta activity in the PaS was phase locked with the CA1 at every depth along the recording track, suggesting that theta-frequency activity was volume-conducted from the hippocampus (D. Caruana, personal communication). To eliminate the contribution of strong volume-conducted activity from the hippocampus and/or EC to the recordings obtained here, theta-frequency EEG activity in the PaS was then recorded using a bipolar electrode. The use of differential recordings from bipolar electrodes effectively removes components of the EEG that are common to both tips, and allows for recording of activity generated at locations between the two tips. Similarly, differential recordings accentuate phase reversals between the two tips, so that locally generated oscillations are amplified when the tips span the layers that generate the oscillations. The amplitude maxima of theta activity was recorded when the leading tip of the electrode was positioned approximately 100-300 μm from the surface of the cortex. This corresponds to the border of layer I/II, so that the electrodes spanned layers II to the middle of layer V or VI. This suggests that theta-frequency activity is generated within layer II/III of the PaS. As the bipolar electrode passed through the superficial layers of the PaS, peak power values were observed across 100-300 μm, corresponding to the thickness of the layer II of the PaS (Funahashi & Stewart, 1997a).

Peak power values in theta range were distributed throughout the superficial layers of the PaS in different animals, however the distribution was sometimes asymmetric, such that larger power values were observed as the leading tip of the bipolar

electrode exited the superficial layers of the Pas, compared to when the leading tip began to enter layers III and II. While it is unclear why some of the tracks demonstrated this pattern, it may be due to slightly stronger active membrane currents in the superficial layers near the soma and proximal dendrites of layer II neurons as compared to below these neurons in layers IV/V. Active currents associated with membrane potential oscillations contribute to local field activity, and may be stronger or more concentrated near the soma and proximal dendrites of the principal cells. In the PaS, superficial cells demonstrate membrane potential oscillations, and this may account for the stronger power values when the leading tip is exiting the parasubicular area, and the lagging tip is still proximal to layers II and I. In addition, excitatory synaptic inputs from the CA1 terminate in layers I and II of the PaS (Kohler, 1985; van Groen & Wyss, 1990a, 1990b). This synaptic input may also accentuate rhythmic field potentials in the superficial layers and result in a slower decline in the amplitude of PaS theta as the electrode moved medially out of layer I. Because of this, the more dorsal tip of the electrode could record relatively strong theta activity from the superficial layers at the same time that the leading tip had exited the PaS. This could result in a slow decline in the amplitude of differentially recorded theta-frequency EEG activity as the bipolar electrode passed out of the PaS.

Due to variation in the position of the CA1 reference electrode, the phase relationship between theta activity in the superficial layers of the PaS and theta activity in the CA1 cannot be defined precisely. Similarly, the exact position of the PaS electrode cannot be precisely localized and, because the phase of theta activity varies with depth in the PaS, variation in the position of the PaS electrode can also affect the phase of the

cross spectrum. However, the approximate phase relationship between PaS and hippocampal theta activity is clear, and it depends systematically on the dorsoventral position of the stationary CA1 reference electrode. In the CA1, theta activity displays a gradual phase shift with laminar depth, in which the apical dendrites of the pyramidal cells in stratum radiatum and stratum lacunosum-moleculare demonstrate an approximate 130°-160° phase reversal with respect to the stratum oriens (Bland, Anderson, & Ganes, 1975; Kowalczyk & Konopacki, 2002; L. W. Leung, 1984). We have found here that theta activity in the superficial layers of the PaS is approximately out of phase with the stratum oriens of the CA1, and is more phase-locked with stratum radiatum or lacunosum-moleculare. The superficial layers of the EC are also known to have a similar phase relation to theta activity in the stratum lacunosum-moleculare (Alonso & Garcia-Austt, 1987a; Buzsaki, 2002; Dickson, Trepel, & Bland, 1994), suggesting that the PaS and EC are largely synchronous in terms of theta activity. Thus, although phase relationships between the EC and the PaS during theta-frequency EEG activity have yet to be directly monitored, it appears that the superficial layers of both the EC and PaS contribute in synchrony to the generation of theta-frequency oscillations. Use of multi-tipped recording electrodes would allow simultaneous recordings at many depths and could help clarify the exact phase relationship between theta activity in the PaS and the EC.

Theta-frequency EEG activity in the PaS is also likely modulated by other, non-CA1 inputs. The anteroventral thalamus has strong connections with the PaS, and cells in this area have been reported to fire rhythmically at theta-frequency. Specifically, cells in the anteroventral thalamus rhythmically burst in synchrony at the peak of theta-frequency

EEG activity recorded in the hippocampus (van Groen & Wyss, 1990b; Vertes, Albo, & Viana Di Prisco, 2001). Cells in the anteroventral thalamus may therefore provide rhythmic inputs synchronized with theta activity in the PaS.

Cholinergic dependence of theta in the PaS

The medial septum is critical for the pacing of theta-frequency EEG activity in the hippocampus and EC (Bland & Oddie, 1998; Bland, Oddie, & Colom, 1999; McNaughton et al., 1977; Petsche, Stumpf, & Gogolak, 1962; Vertes & Kocsis, 1997). Simliarly, the medial septum sends strong projections to the PaS which suggests that the medial septum also plays a critical role in driving theta activity in the PaS (Amaral & Witter, 1989; Gaykema, Luiten, Nyakas, & Traber, 1990; Swanson & Cowan, 1979). Projections from the medial septum include both cholinergic and GABAergic fibers which help to drive theta in the hippocampus (Alonso & Kohler, 1984; Baisden, Woodruff, & Hoover, 1984; Sotty et al., 2003). In the urethane-anesthetized rat, hippocampal theta activity can be blocked by the systemic administration of the muscarinic cholinergic antagonist, atropine (Dickson, Trepel, & Bland, 1994; Kramis, Vanderwolf, & Bland, 1975), indicating that cholinergic inputs from the septum are critical for generating theta activity. We have found here that locally-generated theta activity in the PaS is blocked by systemic administration of atropine (Figure 4), and it is likely that theta in the PaS is mediated, at least in part, by muscarinic inputs from the medial septum.

Identity of cells

The PaS was distinguished from adjacent structures based on the laminar differences between the PaS, EC and the presubiculum. In contrast to layers II/III of

neighboring structures which are very compact, the PaS was identified based its relatively broad band of cells in layers II/III (Amaral & Witter, 1989; Funahashi & Stewart, 1997a; Kohler, 1985; van Groen & Wyss, 1990b). Although it is difficult to distinguish layer II from layer III in the PaS, the sample of recorded cells obtained was situated on the layer I/II border and were clearly from layer II. While the cells were not identified definitively based on cellular morphology, the electrophysiological characteristics of the cells suggested that the majority of these cells were stellate or pyramidal cells. This fits with previous literature on the cell classes found in layer II of the PaS which has reported that cells within the same layers of the PaS tend to be electrophysiologically-homogeneous (Funahashi & Stewart, 1997a, 1997b). Morphologically distinct parasubicular neurons do not show marked differences in electroresponsiveness, and electrophysiological distinctions between cells in the PaS are more apparent between cells located in different layers, such that pyramidal cells in superficial layers are more similar to stellate cells in the superficial layers than to pyramidal cells in deep layers (Funahashi & Stewart, 1997a, 1997b). Both pyramidal and stellate neurons showed voltage-dependent membrane potential oscillations, and it is therefore likely that both cell types contain the voltage-gated conductances for intrinsic membrane potential oscillations that may contribute to the generation of local theta activity.

Membrane potential oscillations are voltage-dependent

Membrane potential oscillations in various regions of the brain are dependent on different ionic mechanisms (Alonso & Llinas, 1989; Llinas & Yarom, 1986). The majority of layer II parasubicular cells show voltage-dependent membrane potential oscillations that are not reliant on synaptic input, and this suggests the involvement of

non-synaptic voltage-dependent conductances. By hyperpolarizing layer II parasubicular cells slightly, the power of oscillations significantly decreased, as did the frequency of the oscillations, which may reflect the fewer number of voltage-gated channels involved in the oscillations at lower voltage levels.

Subthreshold membrane potential oscillations in the PaS may be dependent on voltage-dependent channels. The hyperpolarization-activated time-dependent inward rectifying conductance I_h is responsible for repetitive firing in interneurons in stratum oriens of the CA1 (Maccaferri & McBain, 1996), and may be one conductance that could contribute to subthreshold membrane potential oscillations (Dickson et al., 2000). In addition, the persistent sodium current (I_{NaP}) and a potassium conductance (K^+) have been found to underlie membrane potential oscillations in both hippocampal principal cell and interneuron populations (Chapman & Lacaille, 1999b; Garcia-Munoz, Barrio, & Buno, 1993; L. W. Leung & Yim, 1991), as well as in stellate cells in the superficial layers of the EC (Klink & Alonso, 1993).

Raising bath temperature increases the kinetics of K^+ and Na^+ conductances, and increases the frequency of membrane potential oscillations of hippocampal interneurons to frequencies similar to those observed *in vivo* (Chapman & Lacaille, 1999b; Shen & Schwartzkroin, 1988; Thompson, Masukawa, & Prince, 1985). Increasing the temperature of layer II cells of the PaS to 32° C also significantly increased the frequency of the oscillations from 3.40 to 5.96 Hz, which is similar to the frequencies of theta activity observed *in vivo* without altering the magnitude of oscillations (Bland, 1986; Green & Arduini, 1954; Petsche, Stumpf, & Gogolak, 1962).

Interneurons in layer II of the PaS

Membrane potential oscillations were recorded in 4 additional cells that were putative interneurons. These cells were characterized by high input resistance, short spike-widths, and large afterhyperpolarizations. Interneurons in the hippocampal regions demonstrate voltage-dependent membrane potential oscillations, and are thought to play an integral role in the generation of theta activity by synchronizing principal cells with rhythmic inhibitory input (Chapman & Lacaille, 1999a, 1999b). Theta-frequency firing of GABAergic input from the medial septum inhibits GABAergic interneurons in the stratum oriens, and this causes the rhythmic release of pyramidal cells from tonic inhibition. This provides an additional mechanism by which pyramidal cells may be synchronized by inhibitory interneurons (Cobb, Buhl, Halasy, Paulsen, & Somogyi, 1995; Cobb et al., 1997).

Similar mechanisms may play a substantial role in the generation of theta activity in the PaS by rhythmically disinhibiting principal cells. Anatomical evidence shows that the superficial layers of the PaS contain numerous non-pyramidal and non-stellate GABAergic cells (Kohler, Wu, & Chan-Palay, 1985; Wouterlood, Hartig, Bruckner, & Witter, 1995). Electrophysiological data support the notion that superficial layers of retrohippocampal cortices are under strong inhibitory control (Funahashi & Stewart, 1998; R. S. Jones & Buhl, 1993; R. S. G. Jones, 1990). During theta activity, cholinergic inputs from the septum may depolarize the principal cells of the superficial layers, releasing these cells from local inhibition by muscarinic-dependent receptor activation. Cholinergic inputs may also serve to depolarize local interneurons that could the help

synchronize theta activity in principal cells of the PaS by evoking synchronous, rhythmic inhibitory postsynaptic potentials.

Hippocampal interneurons in the stratum lacunosum-moleculare display intrinsic membrane potential oscillations that are dependent on cholinergic mechanisms. Cholinergic agonism depolarizes entorhinal and hippocampal cells to voltage levels near threshold leading to membrane potential oscillations (Chapman & Lacaille, 1999a; Dickson & Alonso, 1997; Klink & Alonso, 1997). The superficial layers of the PaS also receive cholinergic (van Groen & Wyss, 1990b) from the medial septum, and GABAergic inputs from both local interneurons and septal regions (Kohler, Wu, & Chan-Palay, 1985). Cholinergically-induced depolarization in the PaS may be regulated by both phasic septal inputs and rhythmic local inhibition. Theta activity in the superficial layers of the PaS is therefore likely supported by a number of intrinsic and extrinsic mechanisms, including local inhibitory interneurons, and both cholinergic and GABAergic inputs from the medial septum.

Neurons in superficial layers of the EC, PaS, and presubiculum are known to fire in relation to theta rhythm (Alonso & Garcia-Austt, 1987b; Cacucci, Lever, Wills, Burgess, & O'Keefe, 2004; Chrobak & Buzsaki, 1994) . Furthermore, Funahashi and Stewart (1998) proposed that the output of the PaS may exert phasic inhibition upon target cells in superficial cells of the EC, and consequently influence the generation of theta-frequency activity in the layer II of the EC. Cells in the PaS may therefore contribute to the timing of discharges in the superficial EC cells, and entrain their firing to specific phases of the theta activity in the EC (Chapman & Lacaille, 1999b; Sun, Zhao, Nelson, & Alkon, 2001).

Significance

Theta-frequency EEG activity has been strongly linked to spatial navigation and voluntary movement, yet most of the previous literature has focused on theta activity in the hippocampus proper (Bland & Oddie, 2001; Buzsaki, 2005; Green & Arduini, 1954; Vanderwolf, 1969). Other retrohippocampal structures including the EC and PaS also express theta activity, however little is known about the roles that these areas may play in the integration of information within the entorhinal-hippocampal network.

It is thought that cells in the PaS encode allocentric information about the location and orientation with "place-by-direction cells" (Cacucci, Lever, Wills, Burgess, & O'Keefe, 2004). Unlike place cells, which discharge preferentially in certain locations of an environment, or head-direction cells, which code for the animal's directional heading (Blair, Cho, & Sharp, 1999; Taube, 1995a), place-by-direction cells in the PaS encode information about both location and direction. Thus, the PaS appears to be important for the integration of spatial information from place cells in the hippocampus and head direction information from the anteroventral thalamus. Hargreaves and colleagues (2005) suggest that the PaS may play a critical role in the creation of spatial representations in the EC through integrating information from the anteroventral thalamus and other brains areas associated with spatial processes. This is consistent with the effects of lesions in the PaS, which result in spatial deficits by decreasing the directionality or specificity of hippocampal place cells, likely by disrupting the integration of spatial information in the hippo-entorhinal circuit (Liu, Jarrard, & Bilkey, 2001). Theta activity in the PaS may therefore serve to integrate information from the hippocampus and the anteroventral

thalamus, and supply the EC with integrated spatial information required to support the activity of specialized place cells in the EC.

The output of the PaS is known to cause rapid short-term facilitation or inhibition of responses of neurons in layer II of the EC to activation of inputs from the piriform cortex (Caruana & Chapman, 2004; R. S. G. Jones, 1990). Here, it has been demonstrated that theta-frequency EEG activity may help to synchronize the output of the PaS, and it is possible that this may lead to rhythmic facilitation of EC responses to sensory input during theta-related behaviors (Chapman & Racine, 1997; Huerta & Lisman, 1996a, 1996b). Short-term facilitation affects can promote lasting synaptic plasticity in the EC thought to contribute to learning and memory (Chapman & Racine, 1997). Therefore, by promoting mechanisms of synaptic plasticity, theta activity in the PaS may contribute to long-lasting modifications in how spatial information is processed in the EC, and may contribute to learning about how to effectively navigate through environments.

REFERENCES

Alonso, A., & Garcia-Austt, E. (1987a). Neuronal sources of theta rhythm in the entorhinal cortex of the rat. I. Laminar distribution of theta field potentials. *Exp Brain Res, 67*(3), 493-501.

Alonso, A., & Garcia-Austt, E. (1987b). Neuronal sources of theta rhythm in the entorhinal cortex of the rat. II. Phase relations between unit discharges and theta field potentials. *Exp Brain Res, 67*(3), 502-509.

Alonso, A., & Klink, R. (1993). Differential electroresponsiveness of stellate and pyramidal-like cells of medial entorhinal cortex layer II. *J Neurophysiol, 70*(1), 128-143.

Alonso, A., & Kohler, C. (1984). A study of the reciprocal connections between the septum and the entorhinal area using anterograde and retrograde axonal transport methods in the rat brain. *J Comp Neurol, 225*(3), 327-343.

Alonso, A., & Llinas, R. R. (1989). Subthreshold Na+-dependent theta-like rhythmicity in stellate cells of entorhinal cortex layer II. *Nature, 342*(6246), 175-177.

Amaral, D. G., & Witter, M. P. (1989). The three-dimensional organization of the hippocampal formation: a review of anatomical data. *Neuroscience, 31*(3), 571-591.

Amaral, D. G., & Witter, M. P. (1995). Hippocampal Formation. In G. Paxinos & C. Watson (Eds.), *The rat brain in sterotaxic coordinates* (3rd ed.). San Diego: Academic Press.

Baisden, R. H., Woodruff, M. L., & Hoover, D. B. (1984). Cholinergic and non-cholinergic septo-hippocampal projections: a double-label horseradish peroxidase-acetylcholinesterase study in the rabbit. *Brain Res, 290*(1), 146-151.

Blair, H. T., Cho, J., & Sharp, P. E. (1999). The anterior thalamic head-direction signal is abolished by bilateral but not unilateral lesions of the lateral mammillary nucleus. *J Neurosci, 19*(15), 6673-6683.

Bland, B. H. (1986). The physiology and pharmacology of hippocampal formation theta rhythms. *Prog Neurobiol, 26*(1), 1-54.

Bland, B. H., Anderson, P., & Ganes, T. (1975). Two generators of hippocampal theta activity in rabbits. *Brain Res, 94*(2), 199-218.

Bland, B. H., Colom, L. V., Konopacki, J., & Roth, S. H. (1988). Intracellular records of carbachol-induced theta rhythm in hippocampal slices. *Brain Res, 447*(2), 364-368.

Bland, B. H., Konopacki, J., & Dyck, R. H. (2002). Relationship between membrane potential oscillations and rhythmic discharges in identified hippocampal theta-related cells. *J Neurophysiol, 88*(6), 3046-3066.

Bland, B. H., & Oddie, S. D. (1998). Anatomical, electrophysiological and pharmacological studies of ascending brainstem hippocampal synchronizing pathways. *Neurosci Biobehav Rev, 22*(2), 259-273.

Bland, B. H., & Oddie, S. D. (2001). Theta band oscillation and synchrony in the hippocampal formation and associated structures: the case for its role in sensorimotor integration. *Behav Brain Res, 127*(1-2), 119-136.

Bland, B. H., Oddie, S. D., & Colom, L. V. (1999). Mechanisms of neural synchrony in the septohippocampal pathways underlying hippocampal theta generation. *J Neurosci, 19*(8), 3223-3237.

Bonansco, C., & Buno, W. (2003). Cellular mechanisms underlying the rhythmic bursts induced by NMDA microiontophoresis at the apical dendrites of CA1 pyramidal neurons. *Hippocampus, 13*(1), 150-163.

Buzsaki, G. (2002). Theta oscillations in the hippocampus. *Neuron, 33*(3), 325-340.

Buzsaki, G. (2005). Theta rhythm of navigation: link between path integration and landmark navigation, episodic and semantic memory. *Hippocampus, 15*(7), 827-840.

Buzsaki, G., Leung, L. W., & Vanderwolf, C. H. (1983). Cellular bases of hippocampal EEG in the behaving rat. *Brain Res, 287*(2), 139-171.

Caballero-Bleda, M., & Witter, M. P. (1993). Regional and laminar organization of projections from the presubiculum and parasubiculum to the entorhinal cortex: an anterograde tracing study in the rat. *J Comp Neurol, 328*(1), 115-129.

Caballero-Bleda, M., & Witter, M. P. (1994). Projections from the presubiculum and the parasubiculum to morphologically characterized entorhinal-hippocampal projection neurons in the rat. *Exp Brain Res, 101*(1), 93-108.

Cacucci, F., Lever, C., Wills, T. J., Burgess, N., & O'Keefe, J. (2004). Theta-modulated place-by-direction cells in the hippocampal formation in the rat. *J Neurosci, 24*(38), 8265-8277.

Caplan, J. B., Madsen, J. R., Schulze-Bonhage, A., Aschenbrenner-Scheibe, R., Newman, E. L., & Kahana, M. J. (2003). Human theta oscillations related to sensorimotor integration and spatial learning. *J Neurosci, 23*(11), 4726-4736.

Caruana, D. A., & Chapman, C. A. (2004). Stimulation of the parasubiculum modulates entorhinal cortex responses to piriform cortex inputs in vivo. *J Neurophysiol, 92*(2), 1226-1235.

Chapman, C. A., & Lacaille, J. C. (1999a). Cholinergic induction of theta-frequency oscillations in hippocampal inhibitory interneurons and pacing of pyramidal cell firing. *J Neurosci, 19*(19), 8637-8645.

Chapman, C. A., & Lacaille, J. C. (1999b). Intrinsic theta-frequency membrane potential oscillations in hippocampal CA1 interneurons of stratum lacunosum-moleculare. *J Neurophysiol, 81*(3), 1296-1307.

Chapman, C. A., & Racine, R. J. (1997). Converging inputs to the entorhinal cortex from the piriform cortex and medial septum: facilitation and current source density analysis. *J Neurophysiol, 78*(5), 2602-2615.

Chrobak, J. J., & Buzsaki, G. (1994). Selective activation of deep layer (V-VI) retrohippocampal cortical neurons during hippocampal sharp waves in the behaving rat. *J Neurosci, 14*(10), 6160-6170.

Cobb, S. R., Buhl, E. H., Halasy, K., Paulsen, O., & Somogyi, P. (1995). Synchronization of neuronal activity in hippocampus by individual GABAergic interneurons. *Nature, 378*(6552), 75-78.

Cobb, S. R., Halasy, K., Vida, I., Nyiri, G., Tamas, G., Buhl, E. H., et al. (1997). Synaptic effects of identified interneurons innervating both interneurons and pyramidal cells in the rat hippocampus. *Neuroscience, 79*(3), 629-648.

Denham, M. J., & Borisyuk, R. M. (2000). A model of theta rhythm production in the septal-hippocampal system and its modulation by ascending brain stem pathways. *Hippocampus, 10*(6), 698-716.

Dickson, C. T., & Alonso, A. (1997). Muscarinic induction of synchronous population activity in the entorhinal cortex. *J Neurosci, 17*(17), 6729-6744.

Dickson, C. T., Magistretti, J., Shalinsky, M. H., Fransen, E., Hasselmo, M. E., & Alonso, A. (2000). Properties and role of I(h) in the pacing of subthreshold oscillations in entorhinal cortex layer II neurons. *J Neurophysiol, 83*(5), 2562-2579.

Dickson, C. T., Trepel, C., & Bland, B. H. (1994). Extrinsic modulation of theta field activity in the entorhinal cortex of the anesthetized rat. *Hippocampus, 4*(1), 37-51.

Engel, A. K., Fries, P., & Singer, W. (2001). Dynamic predictions: oscillations and synchrony in top-down processing. *Nat Rev Neurosci, 2*(10), 704-716.

Funahashi, M., & Stewart, M. (1997a). Presubicular and parasubicular cortical neurons of the rat: electrophysiological and morphological properties. *Hippocampus, 7*(2), 117-129.

Funahashi, M., & Stewart, M. (1997b). Presubicular and parasubicular cortical neurons of the rat: functional separation of deep and superficial neurons in vitro. *J Physiol, 501 (Pt 2)*, 387-403.

Funahashi, M., & Stewart, M. (1998). GABA receptor-mediated post-synaptic potentials in the retrohippocampal cortices: regional, laminar and cellular comparisons. *Brain Res, 787*(1), 19-33.

Garcia-Munoz, A., Barrio, L. C., & Buno, W. (1993). Membrane potential oscillations in CA1 hippocampal pyramidal neurons in vitro: intrinsic rhythms and fluctuations entrained by sinusoidal injected current. *Exp Brain Res, 97*(2), 325-333.

Gaykema, R. P., Luiten, P. G., Nyakas, C., & Traber, J. (1990). Cortical projection patterns of the medial septum-diagonal band complex. *J Comp Neurol, 293*(1), 103-124.

Green, J. D., & Arduini, A. A. (1954). Hippocampal electrical activity in arousal. *J Neurophysiol, 17*(6), 533-557.

Hafting, T., Fyhn, M., Molden, S., Moser, M. B., & Moser, E. I. (2005). Microstructure of a spatial map in the entorhinal cortex. *Nature, 436*(7052), 801-806.

Hargreaves, E. L., Rao, G., Lee, I., & Knierim, J. J. (2005). Major dissociation between medial and lateral entorhinal input to dorsal hippocampus. *Science, 308*(5729), 1792-1794.

Hasselmo, M. E. (2005). What is the function of hippocampal theta rhythm?--Linking behavioral data to phasic properties of field potential and unit recording data. *Hippocampus, 15*(7), 936-949.

Huerta, P. T., & Lisman, J. E. (1993). Heightened synaptic plasticity of hippocampal CA1 neurons during a cholinergically induced rhythmic state. *Nature, 364*(6439), 723-725.

Huerta, P. T., & Lisman, J. E. (1996a). Low-frequency stimulation at the troughs of theta-oscillation induces long-term depression of previously potentiated CA1 synapses. *J Neurophysiol, 75*(2), 877-884.

Huerta, P. T., & Lisman, J. E. (1996b). Synaptic plasticity during the cholinergic theta-frequency oscillation in vitro. *Hippocampus, 6*(1), 58-61.

Hyman, J. M., Wyble, B. P., Goyal, V., Rossi, C. A., & Hasselmo, M. E. (2003). Stimulation in hippocampal region CA1 in behaving rats yields long-term potentiation when delivered to the peak of theta and long-term depression when delivered to the trough. *J Neurosci, 23*(37), 11725-11731.

Jones, R. S., & Buhl, E. H. (1993). Basket-like interneurones in layer II of the entorhinal cortex exhibit a powerful NMDA-mediated synaptic excitation. *Neurosci Lett, 149*(1), 35-39.

Jones, R. S., & Heinemann, U. (1988). Synaptic and intrinsic responses of medical entorhinal cortical cells in normal and magnesium-free medium in vitro. *J Neurophysiol, 59*(5), 1476-1496.

Jones, R. S. G. (1990). Synaptic responses of neurones in layer II of the rat medial entorhinal cortex to stimulation of the parasubiculum in vitro. *Proceedings of the physiological society, 426*, 48P.

Judge, S. J., & Hasselmo, M. E. (2004). Theta rhythmic stimulation of stratum lacunosum-moleculare in rat hippocampus contributes to associative LTP at a phase offset in stratum radiatum. *J Neurophysiol, 92*(3), 1615-1624.

Klink, R., & Alonso, A. (1993). Ionic mechanisms for the subthreshold oscillations and differential electroresponsiveness of medial entorhinal cortex layer II neurons. *J Neurophysiol, 70*(1), 144-157.

Klink, R., & Alonso, A. (1997). Muscarinic modulation of the oscillatory and repetitive firing properties of entorhinal cortex layer II neurons. *J Neurophysiol, 77*(4), 1813-1828.

Kohler, C. (1985). Intrinsic projections of the retrohippocampal region in the rat brain. I. The subicular complex. *J Comp Neurol, 236*(4), 504-522.

Kohler, C., Wu, J. Y., & Chan-Palay, V. (1985). Neurons and terminals in the retrohippocampal region in the rat's brain identified by anti-gamma-aminobutyric acid and anti-glutamic acid decarboxylase immunocytochemistry. *Anat Embryol (Berl), 173*(1), 35-44.

Kowalczyk, T., & Konopacki, J. (2002). Depth amplitude and phase profiles of carbachol-induced theta in hippocampal formation slices. *Brain Res Bull, 58*(6), 569-574.

Kramis, R., & Vanderwolf, C. H. (1980). Frequency-specific RSA-like hippocampal patterns elicited by septal, hypothalamic, and brain stem electrical stimulation. *Brain Res, 192*(2), 383-398.

Kramis, R., Vanderwolf, C. H., & Bland, B. H. (1975). Two types of hippocampal rhythmical slow activity in both the rabbit and the rat: relations to behavior and effects of atropine, diethyl ether, urethane, and pentobarbital. *Exp Neurol, 49*(1 Pt 1), 58-85.

Lacaille, J. C., & Schwartzkroin, P. A. (1988). Stratum lacunosum-moleculare interneurons of hippocampal CA1 region. I. Intracellular response characteristics, synaptic responses, and morphology. *J Neurosci, 8*(4), 1400-1410.

Leung, L. S. (1998). Generation of theta and gamma rhythms in the hippocampus. *Neurosci Biobehav Rev, 22*(2), 275-290.

Leung, L. S., Roth, L., & Canning, K. J. (1995). Entorhinal inputs to hippocampal CA1 and dentate gyrus in the rat: a current-source-density study. *J Neurophysiol, 73*(6), 2392-2403.

Leung, L. S., & Shen, B. (2004). Glutamatergic synaptic transmission participates in generating the hippocampal EEG. *Hippocampus, 14*(4), 510-525.

Leung, L. W. (1984). Model of gradual phase shift of theta rhythm in the rat. *J Neurophysiol, 52*(6), 1051-1065.

Leung, L. W., & Buzsaki, G. (1983). Spectral analysis of hippocampal unit train in relation to hippocampal EEG. *Electroencephalogr Clin Neurophysiol, 56*(6), 668-671.

Leung, L. W., & Yim, C. Y. (1991). Intrinsic membrane potential oscillations in hippocampal neurons in vitro. *Brain Res, 553*(2), 261-274.

Liu, P., Jarrard, L. E., & Bilkey, D. K. (2001). Excitotoxic lesions of the pre- and parasubiculum disrupt object recognition and spatial memory processes. *Behav Neurosci, 115*(1), 112-124.

Llinas, R., & Yarom, Y. (1986). Oscillatory properties of guinea-pig inferior olivary neurones and their pharmacological modulation: an in vitro study. *J Physiol, 376*, 163-182.

Maccaferri, G., & McBain, C. J. (1996). The hyperpolarization-activated current (Ih) and its contribution to pacemaker activity in rat CA1 hippocampal stratum oriens-alveus interneurones. *J Physiol, 497 (Pt 1)*, 119-130.

McNaughton, N., James, D., Stewart, J., Gray, J., Valero, I., & Drewnowski, A. (1977). Septal driving of hippocampal theta rhythm as a function of frequency in the male rat: effects of drugs. *Neuroscience, 2*, 1019-1027.

Mitchell, S. J., & Ranck, J. B., Jr. (1980). Generation of theta rhythm in medial entorhinal cortex of freely moving rats. *Brain Res, 189*(1), 49-66.

Natsume, K., Hallworth, N. E., Szgatti, T. L., & Bland, B. H. (1999). Hippocampal theta-related cellular activity in the superior colliculus of the urethane-anesthetized rat. *Hippocampus, 9*(5), 500-509.

Pape, H. C., Pare, D., & Driesang, R. B. (1998). Two types of intrinsic oscillations in neurons of the lateral and basolateral nuclei of the amygdala. *J Neurophysiol, 79*(1), 205-216.

Paxinos, G., & Watson, C. (1998). *The rat brain in stereotaxic coordinates* (4th ed.). San Diego: Academic Press.

Petsche, H., Stumpf, C., & Gogolak, G. (1962). The significance of the rabbit's septum as a relay station between the midbrain and the hippocampus. I. The control of hippocampus arousal activity by the septum cells. *Electroencephalogr Clin Neurophysiol, 14*, 202-211.

Robinson, T. E. (1980). Hippocampal rhythmic slow activity (RSA; theta): a critical analysis of selected studies and discussion of possible species-differences. *Brain Res, 203*(1), 69-101.

Shen, K. F., & Schwartzkroin, P. A. (1988). Effects of temperature alterations on population and cellular activities in hippocampal slices from mature and immature rabbit. *Brain Res, 475*(2), 305-316.

Sotty, F., Danik, M., Manseau, F., Laplante, F., Quirion, R., & Williams, S. (2003). Distinct electrophysiological properties of glutamatergic, cholinergic and GABAergic rat septohippocampal neurons: novel implications for hippocampal rhythmicity. *J Physiol, 551*(Pt 3), 927-943.

Stewart, M., & Wong, R. K. (1993). Intrinsic properties and evoked responses of guinea pig subicular neurons in vitro. *J Neurophysiol, 70*(1), 232-245.

Sun, M. K., Zhao, W. Q., Nelson, T. J., & Alkon, D. L. (2001). Theta rhythm of hippocampal CA1 neuron activity: gating by GABAergic synaptic depolarization. *J Neurophysiol, 85*(1), 269-279.

Swanson, L. W., & Cowan, W. M. (1979). The connections of the septal region in the rat. *J Comp Neurol, 186*(4), 621-655.

Taube, J. S. (1995a). Head direction cells recorded in the anterior thalamic nuclei of freely moving rats. *J Neurosci, 15*(1 Pt 1), 70-86.

Taube, J. S. (1995b). Place cells recorded in the parasubiculum of freely moving rats. *Hippocampus, 5*(6), 569-583.

Thompson, S. M., Masukawa, L. M., & Prince, D. A. (1985). Temperature dependence of intrinsic membrane properties and synaptic potentials in hippocampal CA1 neurons in vitro. *J Neurosci, 5*(3), 817-824.

van Groen, T., & Wyss, J. M. (1990a). Extrinsic projections from area CA1 of the rat hippocampus: olfactory, cortical, subcortical, and bilateral hippocampal formation projections. *J Comp Neurol, 302*(3), 515-528.

van Groen, T., & Wyss, J. M. (1990b). The connections of presubiculum and parasubiculum in the rat. *Brain Res, 518*(1-2), 227-243.

van Vliet, E. A., Aronica, E., Tolner, E. A., Lopes da Silva, F. H., & Gorter, J. A. (2004). Progression of temporal lobe epilepsy in the rat is associated with immunocytochemical changes in inhibitory interneurons in specific regions of the hippocampal formation. *Exp Neurol, 187*(2), 367-379.

Vanderwolf, C. H. (1969). Hippocampal electrical activity and voluntary movement in the rat. *Electroencephalogr Clin Neurophysiol, 26*(4), 407-418.

Vanderwolf, C. H., Leung, L. W., & Cooley, R. K. (1985). Pathways through cingulate, neo- and entorhinal cortices mediate atropine-resistant hippocampal rhythmical slow activity. *Brain Res, 347*(1), 58-73.

Vertes, R. P. (2005). Hippocampal theta rhythm: a tag for short-term memory. *Hippocampus, 15*(7), 923-935.

Vertes, R. P., Albo, Z., & Viana Di Prisco, G. (2001). Theta-rhythmically firing neurons in the anterior thalamus: implications for mnemonic functions of Papez's circuit. *Neuroscience, 104*(3), 619-625.

Vertes, R. P., & Kocsis, B. (1997). Brainstem-diencephalo-septohippocampal systems controlling the theta rhythm of the hippocampus. *Neuroscience, 81*(4), 893-926.

Wouterlood, F. G., Hartig, W., Bruckner, G., & Witter, M. P. (1995). Parvalbumin-immunoreactive neurons in the entorhinal cortex of the rat: localization, morphology, connectivity and ultrastructure. *J Neurocytol, 24*(2), 135-153.

Wouterlood, F. G., Saldana, E., & Witter, M. P. (1990). Projection from the nucleus reuniens thalami to the hippocampal region: light and electron microscopic tracing study in the rat with the anterograde tracer Phaseolus vulgaris-leucoagglutinin. *J Comp Neurol, 296*(2), 179-203.

Wu, K., & Leung, L. S. (1998). Monosynaptic activation of CA3 by the medial perforant path. *Brain Res, 797*(1), 35-41.